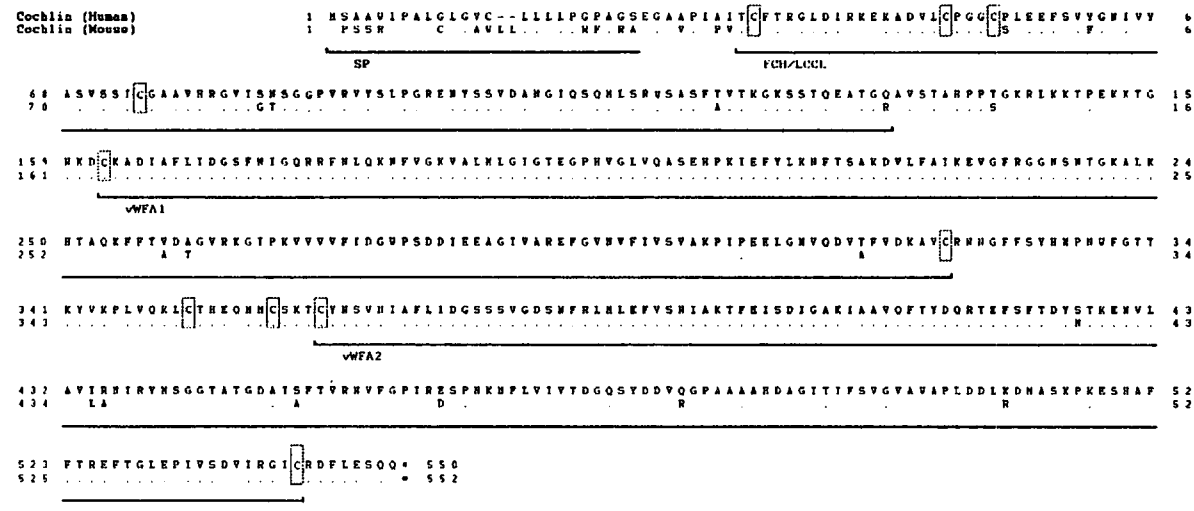

Figure 6. Amino acid sequence of human and mouse cochlin, showing distribution of tryptic digest fragments identified by mass spectrometry from cochlear tissue. The domains of cochlin are underlined and labeled (FCH/LCCL in red, vWFA1 and vWFA2 in blue), as well as the SP, cleaved in mature cochlin and therefore not detected among tryptic fragments. Amino acid residues identical between human and mouse are indicated by a dot. Cochlin peptide coverage, as found in our proteomic analysis from human unaffected formalin-fixed, paraffin-embedded temporal bone sections is highlighted in yellow and from mouse fresh whole cochlear tissue is highlighted in green.

keratins. The intermediate filament, vimentin, is the second most prevalent protein detected in our analysis (29 peptide matches, reflecting 17 unique peptides), followed by collagen type II, alpha 1 (11 peptide matches, representing two unique peptides). Immunohistochemical localization of vimentin in the gerbil inner ear shows high-level expression of this protein in most connective tissue cells and in several different types of epithelial cells, including some types of organ of Corti supporting cells (41).

Our proteomic analysis of formalin-fixed, paraffin-embedded adult human tissue sections has some limitations in the number and complexity of cochlear proteins identified, likely as a result of the inaccessibility and possible degradation of proteins during the extraction process from very small amounts of tissue in 8-μm paraffin sections. However, even with these limitations, many representative proteins were detected. Cochlin is the most prevalent, showing over twice as many detected peptides as vimentin and reflects its high expression and stability even after the processing and extraction protocol from fixed and embedded tissues.

In the proteomic analysis of the DFNA9-affected temporal bone sections (Table 3), there are substantially fewer proteins identified, as well as fewer peptide matches for each protein. However, there is significant overlap in the proteins that were identified in the DFNA9-affected and unaffected samples. Aside from blood components, albumin and α- and β-globins, the major proteins found in the DFNA9-affected temporal bone (and also present in the unaffected sample) are cochlin, collagen types I alpha 1 and alpha 2, and keratins 1 and 2a. A quantitative comparison of proteins across the DFNA9-affected and unaffected samples cannot be made because the two samples varied greatly in complexity and number of total peptide matches for each protein, likely as a result of the greater difficulty of extraction and solubility of proteins in the DFNA9 sections which was apparent during the processing of samples (also discussed below). For every protein identified in the DFNA9 sample, the total number of peptide matches ranges from 1 to 3, whereas in the unaffected sample 1 to 66 matches were found. For instance, in the unaffected sample, the total number of peptide matches are 66 for cochlin, five for keratin 1 and two for collagen type I alpha 2; corresponding peptide matches in the DFNA9-affected sample are three, one and two, respectively. The number of cochlin peptides found in the DFNA9 sample is greater than or equivalent to that for any other protein. Cochlin peptides identified in the DFNA9 sample are from both the N- and C-terminal portions of cochlin spanning amino acid residues 81 to 91, in the FCH/LCCL domain and amino acid residues 526 to 539 in the vWFA2 domain.

One major factor in identification of proteins was that the tissue composition of DFNA9-affected temporal bone samples presented a challenge in total protein extraction due to relative insolubility of these samples. Much of this sample remained as insoluble aggregates during the extraction protocol. Therefore, a large number of proteins were likely not solubilized or extracted, making them inaccessible for mass spectrometry analysis and resulting in lower complexity and number of total proteins as well as a smaller overall number of peptides. The difficulty in extraction and solubility of proteins from DFNA9-affected sections is perhaps not surprising given the observation of the large amounts of DFNA9 eosinophilic aggregates in the spiral ligament and limbus by light microscopy. Nevertheless, cochlin is detected in the DFNA9-affected tissue at least as often as other major proteins such as collagens, keratins and the blood components albumin and globins. Detection of cochlin in the DFNA9 temporal bone as one of the primary proteins identified by proteomic analysis suggests the stability of cochlin aggregates even in the absence and severe degeneration of the fibrocytes that normally express *COCH*, and corroborates our

Table 3. Proteins identified from DFNA9-affected and unaffected adult human temporal bones

Protein name	Accession No.	Unaffected control		DFNA9-affected	
		No. of total peptide matches	No. of unique peptide matches	No. of total peptide matches	No. of unique peptide matches
β-Actin	gi|4501885|	3	2	—	—
Albumin precursor	gi|4502027|	4	4	3	3
Annexin A2; annexin II	gi|4757756|	3	3	—	—
Annexin V; endonexin II	gi|4502107|	5	5	—	—
ATP synthase, mitochondrial F1 complex	gi|4757810|	1	1	—	—
ATPase, alpha 1 polypeptide	gi|21361181|	1	1	—	—
Chondromodulin I precursor	gi|5901932|	1	1	—	
Clusterin	gi|4502905|	7	4	—	—
Cochlin (coagulation factor C homology)	gi|4758022|	66	17	3	2
Collagen type I, alpha 1	gi|4502945|	2	1	3	3
Collagen type I, alpha 2	gi|4502947|	2	2	2	2
Collagen type II, alpha 1, isoform 1	gi|13435125|	11	2	—	—
Collagen type IX, alpha 2	gi|11386161|	3	2	—	—
Collagen type IX, alpha 3	gi|17921995|	1	1	—	—
Collagen type XI, alpha isoform A	gi|18375518|	2	1	—	—
Dermatan sulfate proteoglycan 3	gi|4826704|	1	1	—	—
Desmin	gi|18105050|	3	2	—	—
Eukaryotic translation initiation factor 4A1	gi|30153769|	1	1	—	—
Globin, alpha 2	gi|4504345|	1	1	2	2
β-Globin	gi|4504349|	3	2	3	3
Growth factor receptor-bound protein 10	gi|19923303|	1	1	—	—
Histone H2a	gi|15617199|	1	1	—	—
Histone, H1, member 2	gi|4885375|	2	2	—	—
Histone, H2A, member Q	gi|24638446|	5	4	—	—
Histone, H2A, member Z	gi|4504255|	1	1	—	—
Histone, H2B, member Q	gi|4504277|	2	2	—	—
Histone, H3, family 3A	gi|4504279|	1	1	—	—
Histone, H4, family 2, member N	gi|4504323|	9	6	—	—
Hypothetical protein FLJ10618	gi|8922551|	1	1	—	—
Hypothetical protein LOC221302	gi|21450836|	2	1	—	—
Hypothetical protein XP_298917	gi|29735940|	1	1	—	—
IMP (inosine monophosphate) dehydrogenase 2	gi|30150307|	—	—	1	1
Keratin 1	gi|17318569|	5	5	1	1
Keratin 10	gi|4557697|	3	3	—	—
Keratin 2a	gi|4557703|	2	2	1	1
Keratin 8	gi|30154839|	1	1	—	—
Keratin 9	gi|4557705|	2	2	—	—
Lamin A/C isoform 2	gi|5031875|	2	2	—	—
Lanthionine synthetase C-like protein 1	gi|5174445|	1	1	—	—
Norrin (Norrie disease protein)	gi|4557789|	1	1	—	—
Nuclear ribonucleoprotein A2/B1 isoform A2	gi|4504447|	1	1	—	—
Peroxiredoxin 1	gi|4505591|	3	3	—	—
Peroxiredoxin 2	gi|5902726|	1	1	—	—
Phosphatidylethanolamine-binding protein	gi|18543899|	1	1	—	—
Phosphodiesterase 8A isoform 1	gi|27734721|	1	1	—	—
Plectin 1	gi|4505877|	4	4	—	—
Protease, serine, 1 preproprotein	gi|4506145|	2	1	—	—
Pyruvate kinase, liver and RBC	gi|10835121|	1	1	—	—
Pyruvate kinase, M2 isozyme	gi|29727204|	1	1	—	—
Pyruvate kinase-3	gi|4505839|	2	2	—	—
Ring finger protein 14	gi|4757762|	1	1	—	—
S100 calcium-binding protein, beta	gi|5454034|	1	1	—	—
Similar to natural killer cell transcript 4	gi|30158950|	1	1	—	—
Tolloid-like 1	gi|22547221|	1	1	—	—
Tropomyosin 2, beta	gi|4507649|	1	1	—	—
Tropomyosin 3	gi|24119203|	1	1	—	—
α-Tubulin	gi|30149013|	1	1	—	—
Tumor necrosis factor type 1 receptor	gi|7706485|	1	1	—	—
Ubiquitin and ribosomal protein S27	gi|4506713|	1	1	—	—
Vimentin	gi|4507895|	29	17	—	—
Vinculin isoform VCL	gi|4507877|	1	1	—	—
Vitronectin precursor	gi|18201911|	2	2	—	—

immunohistochemical finding of intense cochlin staining of the abundant deposits found in the DFNA9-affected inner ears.

RT–PCR analysis

To evaluate whether the mutant *COCH* allele in individuals with the P51S mutation (nucleotide C207T) displays stable expression of the mutant *COCH* transcript, reverse transcription–polymerase chain reaction (RT–PCR) was performed on RNA from Epstein-Barr virus (EBV)-transformed cell lines. One distinct band of the expected size was obtained (data not shown) using primers flanking the mutation. Sequence chromatographs show approximately equal peak heights for both the normal and mutated base pairs in the heterozygote DFNA9-affected sample and one single peak of higher amplitude for the normal base pair in the unaffected sample.

These results suggest that the mutant *COCH* transcript shows stable expression in P51S DFNA9 patients and is not subjected to degradation. Given that this missense mutation and all other known *COCH* mutations (seven missense and one in-frame deletion) do not cause any premature termination or truncation of the predicted protein sequence, it may be expected that the mutant allele would show stable expression. However, some missense mutations result in unstable transcripts or proteins, which are subjected to degradation by cellular mechanisms and effectively result in lack of a functional protein. In the case of DFNA9, stable detection of the mutant *COCH* transcript is consistent with the hypothesis of a dominant-negative effect of the mutation in DFNA9 pathology rather than haploinsufficiency of cochlin.

Cochlin deposition in DFNA9

Our previous studies have shown cochlin to be secreted and glycosylated in cultured mammalian cells transfected with full-length *COCH* cDNA (42). As an extracellular glycoprotein, with the FCH/LCCL and vWFA domains, cochlin is likely to bind to, or interact with, other cellular components such as extracellular proteins, glycoproteins and proteoglycans. Such interactions have been shown for other proteins containing these types of domains (43–47). Our light microscopy studies of DFNA9 sections have identified the prominent eosinophilic material as an acellular extracellular homogeneous material. Movats pentachrome staining suggests that this material may contain a mucopolysaccharide-like substance (3). Electron microscopic examination of DNFA9 inner ear sections shows these extracellular deposits to be a highly branched, disarrayed, microfibrillar substance, along with scattered glycosaminoglycan-like granules (48). These observations are consistent with our finding of cochlin immunostaining of the eosinophilic ground substance, suggesting that these aggregates contain extracellularly deposited cochlin. It is also possible that other proteins associated with cochlin may be present and that the nature of these interactions is altered as a result of the presence of mutated cochlin.

In terms of the actual mechanism of the missense mutations leading to misfolding and aggregation of cochlin, several *in vitro* studies have been performed to investigate this possibility. Initial studies of the FCH/LCCL domain of cochlin in bacterial cells showed misfolding of this domain due to several of the known disease-causing mutations and precipitation of the mutant FCH/LCCL peptide during the folding process (49). Our transient transfections of full-length *COCH* with several of the inherited mutations did not reveal any differences in secretion or apparent steady-state levels of cochlin (9,42). Another study corroborated these findings and reported differences in cochlin deposition in the extracellular matrix (ECM) of cultured cells, suggesting altered integration of mutated cochlin into the matrix (50). However, a caveat of *in vitro* studies is the lack of the appropriate extracellular environment of the inner ear. Furthermore, the late-onset and progressive nature of DFNA9 suggests that the effects of mutant cochlin such as aggregation or altered interaction with other ECM components may be a cumulative process. A DFNA9 mouse model would more clearly address long-term and progressive changes in the inner ear as a result of *Coch* mutation and such a model is currently being evaluated in our laboratory.

Possible etiology and pathogenesis of DFNA9

Cochlin immunostaining of eosinophilic aggregates in DFNA9 and the severe atrophy of fibrocytes in the same areas point toward the primary sites where pathological changes are likely to have initiated as a result of *COCH* mutations. Other observations in DFNA9 post-mortem sections are neuroepithelial and neural degeneration in the inner ear. Because cochlin is not expressed in these neuroectodermal structures, it is likely that these changes are secondary to those in mesodermal tissues. The striking reduction and degeneration of fibrocytes and replacement by aggregates throughout the spiral ligament and spiral limbus are in the very same sites as the pathways of K+ recycling from epithelial cells of the organ of Corti back into the endolymphatic scala media compartment (51), indicating a disruption of the integrity of the network of gap junctions that normally exists between these cells and plays a critical role in the ion homeostasis necessary for proper hair cell function. Therefore, a disruption of inner ear ionic balance likely occurs in DFNA9 as a result of the lack of fibrocytes and presence of deposits throughout the areas critical for K+ recycling.

Another observation in both unaffected and DFNA9 inner ears is cochlin immunostaining throughout the osseous spiral lamina and in modiolar areas surrounding neurons and their processes, but not in the neural cell bodies or processes. The detection of cochlin deposits within these neural channels suggests that obstruction of these channels and neuronal damage may also be occurring as a result of mutant cochlin aggregates.

An intriguing finding is immunostaining of perivascular areas in the modiolus and throughout the cochlear duct. Such a finding suggests the possibility that cochlin deposition in perivascular aggregates in organs outside the inner ear is implicated in the high prevalence of vascular disorders that has been found in some P51S DFNA9 kindreds (4), including the one to which the present 67-year-old female individual belonged (52,53). These observations warrant further studies of cochlin expression in extralabyrinthine blood vessels.

Another interesting observation is the lack of any similar histopathological findings between DFNA9-affected temporal bones and those of *Coch* (−/−) mice (at ~5 months of age) (30) (Figs 3 and 5). In fact, these mice, which do not express cochlin, do not show any apparent inner ear abnormalities and any significant hearing loss although later timepoints have yet to be evaluated. Our studies showing cochlin-staining eosinophilic deposits in DFNA9, in addition to the absence of overt pathology in *Coch* (−/−) mice at 5 months of age, are further support that this disorder is not likely due to *COCH* haploinsufficiency, but rather a result of deleterious effects by a 'gain-of-function' molecular mechanism of *COCH* missense mutations.

Cochlin deposits found in glaucoma

Recent proteomic studies have revealed cochlin as the most frequently detected protein by mass spectrometry in the trabecular meshwork (TM) of glaucomatous human eyes, but absent in normal age-matched control donor eyes (54). Immunohistochemistry revealed cochlin-staining deposits co-localizing with mucopolysaccharide substance in the TM around Schlemm's canal in glaucomatous eyes in the human and in the DBA/2J mouse model for glaucoma (54,55). Western blot analysis showed an increase in cochlin levels with increasing age in the human and mouse, along with progression of disease, as well as a parallel decrease in type II collagen, an important component of normal TM. It is hypothesized that the altered architecture of this tissue may cause obstruction of the aqueous flow in the eye (54,55). These studies suggest dysregulation of cochlin expression in a subset of human and mouse glaucomas. The finding of cochlin deposits in these eyes is concomitant with an increase in intraocular pressure and precedes optic nerve damage and ganglion cell degeneration (54,55). Interesting similarities such as cochlin deposition and neuronal damage exist between the findings in glaucoma and in DFNA9; parallel studies will provide insight into cochlin function and its role in disease processes in these two sensory systems.

MATERIALS AND METHODS

Tissues

Mouse tissues were obtained according to the guidelines and protocols approved by the Harvard Medical School Standing Committee on Animals (Boston, MA, USA). Human temporal bones were obtained in accordance with the guidelines established by the Human Research Committees at the Massachusetts Eye and Ear Infirmary (Boston, MA, USA) and the Canisius Wilhelmina Hospital (Nijmegen, the Netherlands).

Postnatal mice (3–6 months of age) were used in this study. Wild-type (+/+) mice were used for assessment of normal histology, cochlin localization and proteomic analysis. *Coch* (−/−) mice, used as negative controls, were a gift of Drs Colin Stewart and Clara Rodriguez (29). Mice were perfused intracardially and tissues fixed in 4% paraformaldehyde. After removal of the stapes from the oval window and piercing of the round window, 4% paraformaldehyde fixative was perfused gently through the cochlea. Inner ears were immersed in fixative for 2–4 h, followed by decalcification in 120 mM ethylenediaminetetraacetic acid (EDTA) for 1 week at room temperature, and embedded in paraffin by standard histologic procedures. Serial sections were obtained at 5–8-μm thickness and used for staining with hematoxylin and eosin (H&E) and for immunohistochemistry. For proteomic analysis, cochlear and vestibular tissues were dissected separately and processed as described in 'Proteomic analysis'.

For human tissues, temporal bones from a 67-year-old female who was a member of a large DFNA9 kindred in the Netherlands segregating the P51S cochlin mutation (5,11) were donated and processed at the Otopathology Laboratory of the Massachusetts Eye and Ear Infirmary, Boston, MA. Post-mortem time for obtaining tissues was 6 h. In this DFNA9 individual, the onset of bilateral sensorineural hearing loss and disequilibrium occurred around age 40 years with progression to profound deafness by age 63, which was documented by audiological evaluation. Vestibular symptoms consisted of gait imbalance, instability in the dark and oscillopsia. Vestibular testing revealed bilateral peripheral vestibular hypofunction. For unaffected controls (with no history of hearing loss), temporal bones obtained from two donors, a 63-year-old female and a 75-year-old male were used. Post-mortem times for obtaining control tissues were 8 and 15 h, respectively. Temporal bones were fixed in 10% formalin, decalcified in EDTA and reduced in size using razor blades to contain only the otic capsule and inner ear. To obtain optimal morphology of sections, one of the DFNA9 temporal bones (left side) was embedded in celloidin, as is standard with temporal bones processed for light microscopic study. Immunostaining is challenging in celloidin-embedded sections, even though there is much better tissue integrity in this medium (Fig. 2); therefore, to facilitate immunohistochemistry, the other temporal bone (right side) was embedded in paraffin. This is the first and only temporal bone from a DFNA9 family member that has been embedded in paraffin to date, thereby facilitating our analyses. For the unaffected controls, the temporal bones from the 63-year-old female were embedded in celloidin, and those from the 75-year-old male in paraffin. Specimens were serially sectioned at a thickness of 20 μm for celloidin and 8 μm for paraffin, and selected sections stained with H&E. Paraffin sections were processed for immunohistochemistry and proteomic analysis as described below.

Immunohistochemistry

Immunostaining was performed using an anti-cochlin antibody generated against a peptide in the vWFA1 domain of cochlin (Fig. 1), corresponding to amino acid residues 163–181 of human cochlin, identical to the residues in murine and bovine cochlin (31). Anti-serum was purified through a protein A sepharose column, followed by peptide-affinity chromatography. This antibody (anti-cochlin/vWFA1 domain) recognizes all three different-sized isoforms of cochlin (Fig. 1).

Immunohistochemistry was performed as previously described (19), except for modifications as described below, including lack of the antigen-retrieval step. Paraffin-embedded sections from postnatal (+/+) and *Coch* (−/−) mice, unaffected control and DFNA9-affected human adult temporal bones were incubated with anti-cochlin/vWFA1 domain

antibody overnight at room temperature, washed and incubated with a secondary biotinylated anti-rabbit IgG (Vector Labs, Burlingame, CA, USA). Immunostaining was visualized by incubation with the Vectastain ABC reagent (Vector Labs) followed by 3,3′-diaminobenzidine (DAB). Sections were not counterstained.

Proteomic analysis

For proteomic analysis in the mouse, membranous cochlear and vestibular labyrinths were dissected separately from approximately 3-month-old (+/+) and *Coch* (−/−) mice. Protein lysates were prepared by incubation of tissues in lysis buffer [2% sodium dodecyl sulfate (SDS), 100 mM ammonium bicarbonate, 10 mM dithiothreitol (DTT), pH 8.5] at 90°C for 10 min, 37°C for 60 min, with subsequent sonication in 0.2% SDS, and incubation at 90°C for 10 min. Three rounds of sonication and boiling were performed, followed by alkylation with 30 mM iodoacetamide. The reaction was quenched with 10 mM DTT and samples were separated by SDS gel electrophoresis in 8–16% polyacrylamide gels. Gels were size-fractionated into four sections, destained with two washes of 50% methanol and 5% acetic acid, followed by three alternating washes of ammonium bicarbonate and acetonitrile. Gel slices were dried and subsequently suspended individually in trypsin (5.5 μg/ml in 50 mM ammonium bicarbonate) prior to incubation at 37°C for 18 h for digestion of proteins. Peptides were extracted with two rinses of 50 mM ammonium bicarbonate and two rinses of 50% acetonitrile and 0.1% formic acid. Samples were prepared for mass spectrometry by lyophilization and rehydration in 5% acetonitrile and 0.1% formic acid.

For proteomic analysis of the adult human inner ear, the only materials available were formalin-fixed, paraffin-embedded tissues. Sections of 8 μm in thickness were used from the same DFNA9-affected temporal bone as used for immunohistochemistry. For a human adult temporal bone control, formalin-fixed, paraffin-embedded, 8 μm thick sections were used from an 85-year-old female with otosclerosis, but showing no inner ear histopathology and with normal cochlear duct structures including the spiral ligament and spiral limbus.

Extraction of proteins from human paraffin-embedded sections was performed by adding heptane and incubating at room temperature for 60 min, followed by the addition of methanol to pellet-extracted proteins. Protein extracts were resolubilized and sonicated in 2% SDS, 100 mM ammonium bicarbonate, 10 mM DTT, pH 8.5. Reduction of proteins was achieved by boiling samples at 90°C for 20 min, followed by incubation at 37°C for 60 min and alkylation in 30 mM iodoacetamide for 60 min at room temperature. Trypsin digestion of proteins and preparation for mass spectrometry were performed as described for the mouse samples.

For mass spectrometry, samples were run on an LCQ DECA XP plus Proteome X workstation (Thermo Electron Corporation, San Jose, CA, USA). Peptide identifications were made using Sequest through the Bioworks Browser 3.1 (Thermo Electron Corporation). Database searches were made using the NCBI RefSeqHuman and RefSeqMurine databases using static carbamidomethyl-modified cysteines and differential oxidized methionines, followed by further searches using differential modifications.

Reverse transcription–polymerase chain reaction

RT–PCR was performed with total RNA isolated from EBV-transformed cell lines from two P51S DFNA9 individuals, using the RNAeasy midi-kit (Qiagen, Leusden, the Netherlands). cDNA synthesis was performed as described (56) and PCR was done for 35 cycles under standard conditions using the following primers flanking the mutation: forward 5′-ACCAGAGGCTTGGACATCAG-3′ in exon 4 and reverse 5′-TTTGAGACTGGATGCCATTG-3′ in exon 5. Amplified products were gel-isolated and sequenced using an ABI PRISM Big Dye Terminator Cycle Sequencing V2 Ready reaction kit and the ABI 3730 DNA sequencing apparatus (Applied Biosystems, Foster City, CA, USA).

SUPPLEMENTARY MATERIAL

Supplementary Material is available at HMG Online. The supplementary figure shows immunohistochemistry performed on human adult temporal bone sections with secondary antibody alone, as a negative control; no staining is detected.

ACKNOWLEDGEMENTS

We are especially grateful to the individuals and their families for donation of temporal bones, and a more detailed description of the P51S DFNA9 histopathology is in preparation for publication. We would like to thank Drs Roderick Bronson and Li Zhang at the Dana Farber/Harvard Cancer Center Rodent Histopathology Core. We also thank Drs Colin Stewart and Clara Rodriguez for their gift of the *Coch* (−/−) mice. This work was supported by NIH/NIDCD grants R01-DC03402 (to C.C.M.), R01-DC0188 and P30-05209 (to M.C.L.), the NIDCD National Temporal Bone, Hearing and Balance Pathology Resource Registry and by Mr Axel Eliasen, and the Health and Labor Sciences Research Grants in Japan (Research on Measures for Intractable Diseases, and Sensory and Communicative Disorders) (to T.I.).

This manuscript is dedicated by Cynthia Morton to the memory of Craig Philip Morton, who passed away on July 9, 2005 from pancreatic cancer, and who upon his death donated his temporal bones to the NIDCD National Temporal Bone, Hearing and Balance Pathology Resource Registry (http://www.tbregistry.org/) having struggled with Meniere's disease during his too short life.

Conflict of Interest statement. None declared.

REFERENCES

1. Van Camp, G. and Smith, R.J.H. (2005) Hereditary hearing loss homepage. URL: http://www.webhost.ua.ac.be/hhh/.
2. Halpin, C., Khetarpal, U. and McKenna, M. (1996) Autosomal dominant progressive sensorineural hearing loss in a large North American Family. *Am. J. Audiol.*, **5**, 105–111.

3. Khetarpal, U., Schuknecht, H.F., Gacek, R.R. and Holmes, L.B. (1991) Autosomal dominant sensorineural hearing loss: pedigrees, audiologic and temporal bone findings in two kindreds. *Arch. Otolaryngol. Head Neck Surg.*, **117**, 1032–1042.
4. Bom, S.J.H., Kemperman, M.H., De Kok, Y.J.M., Huygen, P.L.M., Verhagen, W.I.M., Cremers, F.P.M. and Cremers, C.W.R.J. (1999) Progressive cochleovestibular impairment caused by a point mutation in the *COCH* gene at DFNA9. *Laryngoscope*, **109**, 1525–1530.
5. Verhagen, W.I.M., Bom, S.J.H., Huygen, P.L.M., Fransen, E., Van Camp, G. and Cremers, C.W.R.J. (2000) Familial progressive vestibulocochlear dysfunction caused by a *COCH* mutation (DFNA9). *Arch. Neurol.*, **57**, 1045–1047.
6. Verstreken, M., Declau, F., Wuyts, F.L., D'Haese, P., Van Camp, G., Fransen, E., Van den Hauwe, L., Buyle, S., Smets, R.E., Feenstra, L. *et al.* (2001) Hereditary otovestibular dysfunction and Meniere's disease in a large Belgian family is caused by a missense mutation in the *COCH* gene. *Otol. Neurotol.*, **22**, 874–881.
7. Kemperman, M.H., Bom, S.J.H., Lemaire, F.X., Verhagen, W.I.M., Huygen, P.L.M. and Cremers, C.W.R.J. (2002) DFNA9/*COCH* and its phenotype. *Adv. Otorhinolaryngol.*, **61**, 66–72.
8. Lemaire, F.X., Feenstra, L., Huygen, P.L.M., Fransen, E., Devriendt, K., Van Camp, G., Vantrappen, G. and Cremers, C.W.R.J. (2003) Progressive late-onset sensorineural hearing loss and vestibular impairment with vertigo (DFNA9/*COCH*): longitudinal analyses in a Belgian family. *Otol. Neurotol.*, **24**, 743–748.
9. Street, V.A., Kallman, J.C., Robertson, N.G., Kuo, S.F., Morton, C.C. and Phillips, J.O. (2005) A novel DFNA9 mutation in the vWFA2 domain of *COCH* alters a conserved cysteine residue and intrachain disulfide bond formation, resulting in progressive hearing loss and site-specific vestibular and central oculomotor dysfunction. *Am. J. Med. Genet. A*, **139**, 86–95.
10. Robertson, N.G., Lu, L., Heller, S., Merchant, S.N., Eavey, R.D., McKenna, M., Nadol, J.B., Jr, Miyamoto, R.T., Linthicum, F.H., Jr, Lubianca Neto, J.F. *et al.* (1998) Mutations in a novel cochlear gene cause DFNA9, a human nonsyndromic deafness with vestibular dysfunction. *Nat. Genet.*, **20**, 299–303.
11. de Kok, Y.J.M., Bom, S.J.H., Brunt, T.M., Kemperman, M.H., van Beusekom, E., van der Velde-Visser, S.D., Robertson, N.G., Morton, C.C., Huygen, P.L.M., Verhagen, W.I.M. *et al.* (1999) A Pro51Ser mutation in the *COCH* gene is associated with late onset autosomal dominant progressive sensorineural hearing loss with vestibular defects. *Hum. Mol. Genet.*, **8**, 361–366.
12. Fransen, E., Verstreken, M., Verhagen, W.I.M., Wuyts, F.L., Huygen, P.L.M., D'Haese, P., Robertson, N.G., Morton, C.C., McGuirt, W.T., Smith, R.J.H. *et al.* (1999) High prevalence of symptoms of Meniere's disease in three families with a mutation in the *COCH* gene. *Hum. Mol. Genet.*, **8**, 1425–1429.
13. Kamarinos, M., McGill, J., Lynch, M. and Dahl, H. (2001) Identification of a novel *COCH* mutation, I109 N, highlights the similar clinical features observed in DFNA9 families. *Hum. Mutat.*, **17**, 351.
14. Kemperman, M.H., De Leenheer, E.M.R., Huygen, P.L.M., van Duijnhoven, G., Morton, C.C., Robertson, N.G., Cremers, F.P.M., Kremer, H. and Cremers, C.W.R.J. (2005) Audiometric, vestibular, and genetic aspects of a DFNA9 family with a G88E *COCH* mutation. *Otol. Neurotol.*, **26**, 926–933.
15. Usami, S., Takahashi, K., Yuge, I., Ohtsuka, A., Namba, A., Abe, S., Fransen, E., Patthy, L., Otting, G. and Van Camp, G. (2003) Mutations in the *COCH* gene are a frequent cause of autosomal dominant progressive cochleo-vestibular dysfunction, but not of Meniere's disease. *Eur. J. Hum. Genet.*, **11**, 744–748.
16. Nagy, I., Horvath, M., Trexler, M., Repassy, G. and Patthy, L. (2004) A novel *COCH* mutation, V104del, impairs folding of the LCCL domain of cochlin and causes progressive hearing loss. *J. Med. Genet.*, **41**, e9.
17. Robertson, N.G., Khetarpal, U., Gutiérrez-Espeleta, G.A., Bieber, F.R. and Morton, C.C. (1994) Isolation of novel and known genes from a human fetal cochlear cDNA library using subtractive hybridization and differential screening. *Genomics*, **23**, 42–50.
18. Robertson, N.G., Skvorak, A.B., Yin, Y., Weremowicz, S., Johnson, K.R., Kovatch, K.A., Battey, J.F., Bieber, F.R. and Morton, C.C. (1997) Mapping and characterization of a novel cochlear gene in human and in mouse: a positional candidate gene for a deafness disorder, DFNA9. *Genomics*, **46**, 345–354.
19. Robertson, N.G., Resendes, B.L., Lin, J.S., Lee, C., Aster, J.C., Adams, J.C. and Morton, C.C. (2001) Inner ear localization of mRNA and protein products of *COCH*, mutated in the sensorineural deafness and vestibular disorder, DFNA9. *Hum. Mol. Genet.*, **10**, 2493–2500.
20. Ikezono, T., Shindo, S., Ishizaki, M., Li, L., Tomiyama, S., Takumida, M., Pawankar, R., Watanabe, A., Saito, A. and Yagi, T. (2005) Expression of cochlin in the vestibular organ of rats. *ORL J. Otorhinolaryngol. Relat. Spec.*, **67**, 252–258.
21. Ikezono, T., Omori, A., Ichinose, S., Pawankar, R., Watanabe, A. and Yagi, T. (2001) Identification of the protein product of the *Coch* gene (hereditary deafness gene) as the major component of bovine inner ear protein. *Biochim. Biophys. Acta*, **1535**, 258–265.
22. Merchant, S.N., Linthicum, F.H. and Nadol, J.B., Jr (2000) Histopathology of the inner ear in DFNA9. *Adv. Otorhinolaryngol.*, **56**, 212–217.
23. Selkoe, D.J. (2004) Cell biology of protein misfolding: the examples of Alzheimer's and Parkinson's diseases. *Nat. Cell Biol.*, **6**, 1054–1061.
24. Davies, S.W., Turmaine, M., Cozens, B.A., DiFiglia, M., Sharp, A.H., Ross, C.A., Scherzinger, E., Wanker, E.E., Mangiarini, L. and Bates, G.P. (1997) Formation of neuronal intranuclear inclusions underlies the neurological dysfunction in mice transgenic for the HD mutation. *Cell*, **90**, 537–548.
25. Zoghbi, H.Y. and Orr, H.T. (2000) Glutamine repeats and neurodegeneration. *Annu. Rev. Neurosci.*, **23**, 217–247.
26. Waelter, S., Boeddrich, A., Lurz, R., Scherzinger, E., Lueder, G., Lehrach, H. and Wanker, E.E. (2001) Accumulation of mutant huntingtin fragments in aggresome-like inclusion bodies as a result of insufficient protein degradation. *Mol. Biol. Cell*, **12**, 1393–1407.
27. Masliah, E., Rockenstein, E., Veinbergs, I., Mallory, M., Hashimoto, M., Takeda, A., Sagara, Y., Sisk, A. and Mucke, L. (2000) Dopaminergic loss and inclusion body formation in alpha-synuclein mice: implications for neurodegenerative disorders. *Science*, **287**, 1265–1269.
28. Khetarpal, U. (1993) Autosomal dominant sensorineural hearing loss: further temporal bone findings. *Arch. Otolaryngol. Head Neck Surg.*, **119**, 106–108.
29. Rodriguez, C.I., Cheng, J.G., Liu, L. and Stewart, C.L. (2004) Cochlin, a secreted von Willebrand factor type a domain-containing factor, is regulated by leukemia inhibitory factor in the uterus at the time of embryo implantation. *Endocrinology*, **145**, 1410–1418.
30. Makishima, T., Rodriguez, C.I., Robertson, N.G., Morton, C.C., Stewart, C.L. and Griffith, A.J. (2005) Targeted disruption of mouse *Coch* provides functional evidence that DFNA9 hearing loss is not a *COCH* haploinsufficiency disorder. *Hum. Genet.*, **118**, 29–34.
31. Ikezono, T., Shindo, S., Li, L., Omori, A., Ichinose, S., Watanabe, A., Kobayashi, T., Pawankar, R. and Yagi, T. (2004) Identification of a novel Cochlin isoform in the perilymph: insights to Cochlin function and the pathogenesis of DFNA9. *Biochem. Biophys. Res. Commun.*, **314**, 440–446.
32. Skvorak, A.B., Weng, Z., Yee, A.J., Robertson, N.G. and Morton, C.C. (1999) Human cochlear expressed sequence tags provide insight into cochlear gene expression and identify candidate genes for deafness. *Hum. Mol. Genet.*, **8**, 439–452.
33. Boulassel, M.R., Deggouj, N., Tomasi, J.P. and Gersdorff, M. (2001) Inner ear autoantibodies and their targets in patients with autoimmune inner ear diseases. *Acta Otolaryngol.*, **121**, 28–34.
34. Boulassel, M.R., Tomasi, J.P., Deggouj, N. and Gersdorff, M. (2001) *COCH5B2* is a target antigen of anti-inner ear antibodies in autoimmune inner ear diseases. *Otol. Neurotol.*, **22**, 614–618.
35. Kommareddi, P.K., Nair, T.S. and Carey, T.E. (2003) Cochlin is expressed in the supporting cells of the organ of Corti and co-precipitates with CTL2. ARO abstracts 26:58. Presented at the 25th midwinter research meeting of the Association for Research in Otolaryngology, Daytona Beach, FL, February 23–27, 2003.
36. Nair, T.S., Kozma, K.E., Hoefling, N.L., Kommareddi, P.K., Ueda, Y., Gong, T.W., Lomax, M.I., Lansford, C.D., Telian, S.A., Satar, B. *et al.* (2004) Identification and characterization of choline transporter-like protein 2, an inner ear glycoprotein of 68 and 72 kDa that is the target of antibody-induced hearing loss. *J. Neurosci.*, **24**, 1772–1779.
37. Solares, C.A., Edling, A.E., Johnson, J.M., Baek, M.J., Hirose, K., Hughes, G.B. and Tuohy, V.K. (2004) Murine autoimmune hearing loss mediated by CD4+ T cells specific for inner ear peptides. *J. Clin. Invest.*, **113**, 1210–1217.

38. Billings, P. (2004) Experimental autoimmune hearing loss. *J. Clin. Invest.*, **113**, 1114–1117.
39. Back, M.J., Park, H.M., Johnson, J.M., Altuntas, C.Z., Jaini, R., Thomas, D.M., Ball, E.J., Robertson, N.G., Morton, C.C., Hughes, G.B. *et al.* (2006) Increased frequencies of cochlin-specific T cells in patients with autoimmune sensorineural hearing loss. *J. Immunol.*, in press.
40. Palmer-Toy, D.E., Krastins, B., Sarracino, D.A., Nadol, J.B., Jr and Merchant, S.N. (2005) Efficient method for the proteomic analysis of fixed and embedded tissues. *J. Proteome Res.*, **4**, 2404–2411.
41. Schulte, B.A. and Adams, J.C. (1989) Immunohistochemical localization of vimentin in the gerbil inner ear. *J. Histochem. Cytochem.*, **37**, 1787–1797.
42. Robertson, N.G., Hamaker, S.A., Patriub, V., Aster, J.C. and Morton, C.C. (2003) Subcellular localisation, secretion, and post-translational processing of normal cochlin, and of mutants causing the sensorineural deafness and vestibular disorder, DFNA9. *J. Med. Genet.*, **40**, 479–486.
43. Colombatti, A. and Bonaldo, P. (1991) The superfamily of proteins with von Willebrand factor type A-like domains: one theme common to components of extracellular matrix, hemostasis, cellular adhesion, and defense mechanisms. *Blood*, **77**, 2305–2315.
44. Colombatti, A., Bonaldo, P. and Doliana, R. (1993) Type A modules: interacting domains found in several non-fibrillar collagens and in other extracellular matrix proteins. *Matrix*, **13**, 297–306.
45. Lee, J.O., Rieu, P., Arnaout, M.A. and Liddington, R. (1995) Crystal structure of the A domain from the alpha subunit of integrin CR3 (CD11b/CD18). *Cell*, **80**, 631–638.
46. Delrieu, I., Waller, C.C., Mota, M.M., Grainger, M., Langhorne, J. and Holder, A.A. (2002) PSLAP, a protein with multiple adhesive motifs, is expressed in *Plasmodium falciparum* gametocytes. *Mol. Biochem. Parasitol.*, **121**, 11–20.
47. Whittaker, C.A. and Hynes, R.O. (2002) Distribution and evolution of von Willebrand/integrin A domains: widely dispersed domains with roles in cell adhesion and elsewhere. *Mol. Biol. Cell*, **13**, 3369–3387.
48. Khetarpal, U. (2000) DFNA9 is a progressive audiovestibular dysfunction with a microfibrillar deposit in the inner ear. *Laryngoscope*, **110**, 1379–1384.
49. Liepinsh, E., Trexler, M., Kaikkonen, A., Weigelt, J., Banyai, L., Patthy, L. and Otting, G. (2001) NMR structure of the LCCL domain and implications for DFNA9 deafness disorder. *EMBO J.*, **20**, 5347–5353.
50. Grabski, R., Szul, T., Sasaki, T., Timpl, R., Mayne, R., Hicks, B. and Sztul, E. (2003) Mutations in *COCH* that result in non-syndromic autosomal dominant deafness (DFNA9) affect matrix deposition of cochlin. *Hum. Genet.*, **113**, 406–416.
51. Steel, K.P. (1999) Perspectives: biomedicine. The benefits of recycling. *Science*, **285**, 1363–1364.
52. Verhagen, W.I.M., Huygen, P.L.M., Theunissen, E.J.J.M. and Joosten, E.M.G. (1989) Hereditary vestibulo-cochlear dysfunction and vascular disorders. *J. Neurol. Sci.*, **92**, 55–63.
53. Verhagen, W.I.M., Bom, S.J.H., Fransen, E., Van Camp, G., Huygen, P.L.M., Theunissen, E.J.J.M. and Cremers, C.W.R.J. (2001) Hereditary cochleovestibular dysfunction due to a *COCH* gene mutation (DFNA9): a follow-up study of a family. *Clin. Otolaryngol. Allied Sci.*, **26**, 477–483.
54. Bhattacharya, S.K., Rockwood, E.J., Smith, S.D., Bonilha, V.L., Crabb, J.S., Kuchtey, R.W., Robertson, N.G., Peachey, N.S., Morton, C.C. and Crabb, J.W. (2005) Proteomics reveal Cochlin deposits associated with glaucomatous trabecular meshwork. *J. Biol. Chem.*, **280**, 6080–6084.
55. Bhattacharya, S.K., Annangudi, S.P., Salomon, R.G., Kuchtey, R.W., Peachey, N.S. and Crabb, J.W. (2005) Cochlin deposits in the trabecular meshwork of the glaucomatous DBA/2J mouse. *Exp. Eye Res.*, **80**, 741–744.
56. Luijendijk, M.W., van de Pol, T.J., van Duijnhoven, G., den Hollander, A.I., ten Caat, J., van Limpt, V., Brunner, H.G., Kremer, H. and Cremers, F.P. (2003) Cloning, characterization, and mRNA expression analysis of novel human fetal cochlear cDNAs. *Genomics*, **82**, 480–490.

The Laryngoscope
Lippincott Williams & Wilkins, Inc.

Cochlear Protection by Local Insulin-Like Growth Factor-1 Application Using Biodegradable Hydrogel

Koji Iwai, MD; Takayuki Nakagawa, MD, PhD; Tsuyoshi Endo, MD; Yoshinori Matsuoka; Tomoko Kita, PhD; Tae-Soo Kim, MD, PhD; Yasuhiko Tabata, PhD; Juichi Ito, MD, PhD

Objective: **The aim of this experimental study was to examine the potential of local recombinant human insulin-like growth factor-1 (rhIGF-1) application through a biodegradable hydrogel for the treatment of cochleae.** ***Methods:*** **A hydrogel immersed with rhIGF-1 was placed on the round window membrane of Sprague-Dawley rats while a hydrogel immersed with physiological saline was applied to control animals. On day 3 after drug application, the animals were exposed to white noise at 120 dB sound pressure level (SPL) for 2 hours. Cochlear function was monitored using measurements of auditory brain stem responses (ABRs) at frequencies of 8, 16, and 32 kHz. The temporal bones were collected 7 or 30 days after noise exposure and the loss of hair cells was quantitatively analyzed.** ***Results:*** **Local rhIGF-1 treatment significantly reduced the elevation of ABR thresholds on days 7 and 30 after noise exposure. Histologic analysis revealed that local rhIGF-1 treatment significantly prohibited the loss of outer hair cells.** ***Conclusions:*** **These findings demonstrate that local IGF-1 application through the biodegradable hydrogel has the potential for protection of cochleae from noise trauma.** ***Key Words:*** **Drug delivery, cochlea, hair cell, protection, growth factor, acoustic trauma, rat.**
Laryngoscope, **116:529–533, 2006**

INTRODUCTION

In recent years, there has been increasing interest in the treatment of inner ear disorders using the local, rather than systemic, application of therapeutic agents, because the former has fewer side effects and is more target-specific. The establishment of clinically applicable strategies for the local application of therapeutic agents should therefore open a new window for the treatment of inner ear disorders. For methods of drug delivery to be viable in clinical settings, it is crucial for the procedure to be technically undemanding and as minimally invasive as possible. Based on such a background, the use of biodegradable polymers for cochlear drug delivery has been investigated.[1–3] Biodegradable polymers, which enable the sustained release of drugs to the cochlear fluid space, can be applied through an intratympanic injection. Among biodegradable polymers, we have reported the efficacy of the biodegradable hydrogel, which is made from porcine type-I collagen, for delivery of brain-derived neurotrophic factor (BDNF) into the cochlear fluid and successful protection of spiral ganglion neurons (SGNs) from degeneration as a result of the loss of cochlear hair cells.[3]

Insulin-like growth factor-1 (IGF-1) is a mitogenic peptide that plays essential roles in the regulation of growth and development in various parts of the body, including the inner ear.[4] IGF-1 is also known to be a neuroprotective agent.[5] In addition, previous studies on the inner ear have suggested the possibility of inner ear protection by IGF-1.[6,7] Moreover, recombinant human IGF-1 (rhIGF-1) has already been approved for clinical use. Our ultimate goal is for local neurotrophin application to be clinically approved for the treatment of inner ears. In the present study, we then selected rhIGF-1 as a suitable neurotrophin for local application to the cochlea using a biodegradable hydrogel as a vehicle for drug delivery. We evaluated whether the application of rhIGF-1 in this manner was effective in protecting against noise-induced hearing loss.

From the Department of Otolaryngology–Head and Neck Surgery (K.I., T.N., T.E., Y.M., T.K., T.-S.K., J.I.), Graduate School of Medicine and the Institute for Frontier Medical Science (Y.T.), Kyoto University, Kyoto, Japan.

Editor's Note: This Manuscript was accepted for publication December 5, 2005.

This study was supported by a Grant-in-Aid for Regenerative Medicine Realization from the Ministry of Education, Science, Sports, Culture and Technology of Japan.

Send Correspondence to Dr. Takayuki Nakagawa, Department of Otolaryngology–Head and Neck Surgery, Graduate School of Medicine, Kyoto University, Kawaharacho 54, Shogoin, Sakyo-ku, 606-8507 Kyoto, Japan. E-mail: tnakagawa@ent.kuhp.kyoto-u.ac.jp

DOI: 10.1097/01.mlg.0000200791.77819.eb

MATERIALS AND METHODS

Experimental Animals

Sprague-Dawley rats (Japan SLC Inc., Hamamatsu, Japan) at 10 weeks of age were used as experimental animals. The Animal Research Committee of the Graduate School of Medicine, Kyoto University, Japan, approved all experimental protocols. Animal care was conducted under the supervision of the Institute of Laboratory Animals at the Graduate School of Medicine, Kyoto University. All experimental procedures were performed in accordance with the U.S. National Institutes of Health guidelines for the care and use of laboratory animals.

Preparation of Hydrogels

The biodegradable hydrogels were prepared as described previously.[8] Briefly, the gels were generated by the glutaraldehyde crosslinking of porcine type-I collagen (Gunze, Ayabe, Japan). The rates of degradation were determined according to the concentration of glutaraldehyde. The present study used a hydrogel that was made with 60 mol/L glutaraldehyde, which could release basic fibroblast growth factor[8] and BDNF[3] for 7 days in vivo.

Local Application of Insulin-Like Growth Factor-1

RhIGF-1 was provided by Astellas Pharma Inc., Tokyo, Japan. After measuring the auditory brain stem responses (ABRs), the otic bulla of the left temporal bone was exposed using a retroauricular approach under general anesthesia with ketamine (100 mg/kg intramuscularly [IM]; Sankyo Co., Tokyo, Japan) and xylazine (9 mg/kg IM; Bayer, Tokyo, Japan). A small hole was made on the left bulla to expose the round window niche. A hydrogel in dry condition was cut into the size of 2 mm^3 under the microscope and immersed with rhIGF-1 (400 μg dissolved in 40 μL physiological saline) 30 minutes before application. The hydrogel was then placed on the round window membrane (RWM) of the IGF group animals (n = 10). The animals applied a hydrogel-immersed physiological saline were used as controls (n = 10).

Noise Exposure and Measurement of Hearing

On day 3 after the IGF-1 application, we measured the ABRs to eliminate animals that showed threshold shifts of more than 10 dB at any frequencies from the experiments. In consequence, no animals showed threshold shifts over 10 dB after local drug application in the present study. The animals were then exposed to white noise at 120 dB sound pressure level (SPL) for 2 hours in a ventilated sound exposure chamber. The sound levels were monitored and calibrated at multiple locations within the sound chamber to ensure uniformity of the stimulus.

Auditory function was assessed by recording ABRs. The measurements of ABR thresholds were performed at frequencies of 8, 16, and 32 kHz before noise exposure and days 7 and 30 after noise exposure. Animals were anesthetized with ketamine (100 mg/kg) and xylazine (9 mg/kg) and kept warm with a heating pad. Generation of acoustic stimuli and subsequent recording of evoked potentials were performed using a PowerLab/4sp (AD Instruments, Castle Hill, Australia). Acoustic stimuli, consisting of tone-burst stimuli (0.1 ms cos^2 rise/fall and 1-ms plateau), were delivered monaurally through a speaker (ES1spc; Bioresearch Center, Nagoya, Japan) connected to a funnel fitted into the external auditory meatus. To record bioelectrical potentials, subdermal stainless steel needle electrodes were inserted at the vertex (ground), ventrolateral to the measured ear (active) and contralateral to the measured ear (reference). Stimuli were calibrated against a ¼-inch free-field microphone (ACO-7016; ACO Pacific, Inc., Belmont, CA) connected to an oscilloscope (DS-8812 DS-538; Iwatsu Electric, Tokyo, Japan) or a sound level meter (LA-5111; Ono Sokki, Yokohama, Japan). The responses between the vertex and mastoid subcutaneous electrodes were amplified with a digital amplifier (MA2; Tucker-Davis Technologies, Alachua, FL). Thresholds were determined from a set of responses at varying intensities with 5-dB SPL intervals and electrical signals were averaged for 1024 repetitions. Thresholds at each frequency were verified at least twice.

Histologic Analysis

On day 7 or 30 after noise exposure, five cochleae from each experimental group were provided for histologic analysis. The animals were anesthetized with ketamine and xylazine, and the left cochleae were exposed. After removal of otic vesicles, 4% paraformaldehyde in 0.01 mol/L phosphate-buffered saline (PBS)

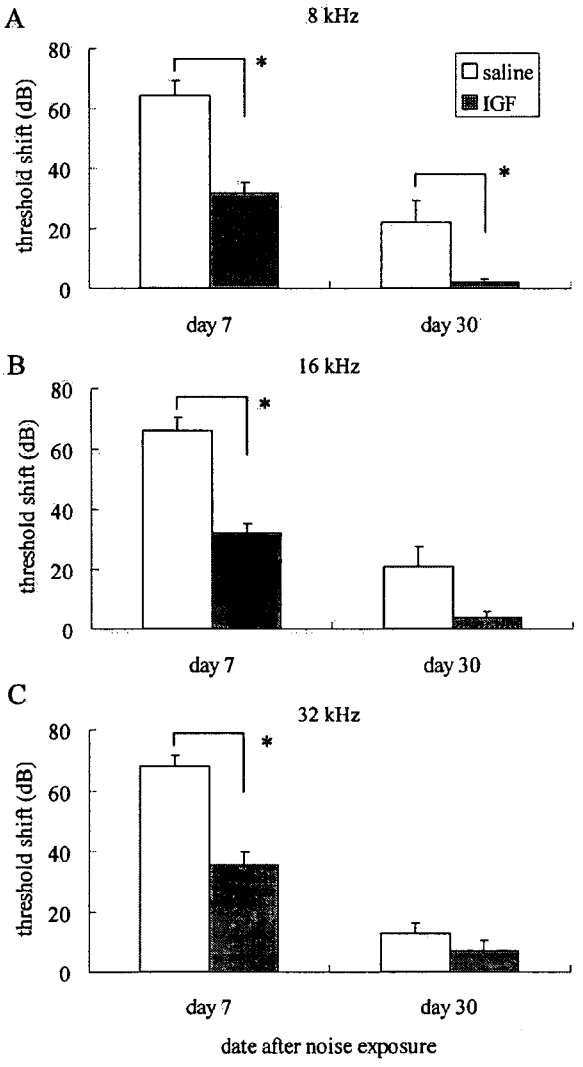

Fig. 1. Auditory brain response threshold shifts for recombinant human insulin-like growth factor-1- (rhIGF-1) and saline-treated cochleae at 8, 16, and 32 kHz on days 7 and 30 after noise exposure. An overall effect of local rhIGF-1 treatment is significant at 8, 16, or 32 kHz (two factorial analysis of variance). Asterisks are indicated significant differences in pairwise comparisons with Fisher's protected least-significant difference. Bars represent standard error (SE).

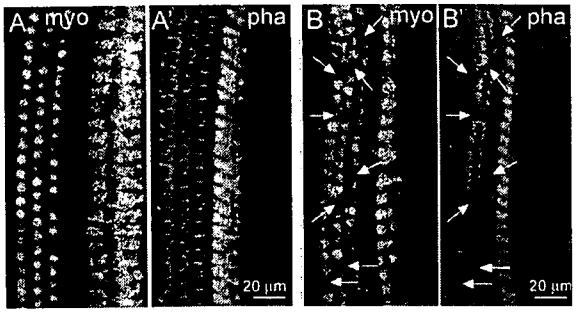

Fig. 2. Photomicrographs of surface preparations stained with myosin VIIa and phalloidin from the second turn of cochleae treated with recombinant human insulin-like growth factor-1 (**A**) or physiological saline (**B**) on day 30. Figures A and B show immunostaining for myosin VIIa (myo), and Figures A' and B' show F-actin labeling by phalloidin. Arrows indicate missing outer hair cells.

at pH 7.4 was gently introduced into the perilymphatic space of the cochleae. The temporal bones were then excised and immersed in the same fixative at 4°C for 12 hours. After rinses with PBS, the cochleae were dissected from the temporal bones and subjected to histologic analysis in whole mounts. We used three regions of cochlear sensory epithelia at a distance of 30% to 40% (apical), 50% to 60% (middle) or 80% to 90% (basal) from the apex for quantitative assessments of hair cell loss.

Immunohistochemistry for myosin VIIa and F-actin labeling by phalloidin were used to label the surviving inner hair cells (IHCs) and outer hair cells (OHCs). Anti-myosin VIIa rabbit polyclonal antibody (1:300; a gift from Tama Hasson, San Diego, CA) was used as the primary antibody, and Alexa-594-conjugated antirabbit goat IgG (1:400; Molecular Probe, Eugene, OR) was used as the secondary antibody. After immunostaining for myosin VIIa, specimens were stained with FITC-conjugated phalloidin (1:300; Molecular Probe). Specimens were viewed using a Leica TCS SP2 confocal microscope (Leica Microsystems Inc., Wetzlar, Germany). Nonspecific labeling was tested by omitting the primary antibody from the staining procedures. We counted the numbers of IHCs and OHCs in 0.2-mm long regions of the apical, middle, or basal portion of cochleae, respectively.

Statistical Analyses

An overall effect on ABR threshold shifts of application of rhIGF-1 was examined by the two-way factorial analysis of variance. When the interaction was significant, multiple comparisons with Fisher's protected least-significant difference (PLSD) were used for pairwise comparisons. The differences in OHC numbers in each region of the cochlea between the rhIGF-1- and saline-treated cochleae were examined using the Student t test. A P value less than .05 was considered statistically significant. Values are expressed as the mean ± standard error.

RESULTS

Functional Protection

The time course of alterations in ABR threshold shifts after noise exposure at 8, 16, or 32 kHz is shown in Figure 1. Local rhIGF-1 treatment demonstrated significant effects on ABR threshold shifts at each frequency. An overall effect on data for 8 kHz of rhIGF-1 application was significant ($P < .001$). The differences in threshold shifts between rhIGF-1- and saline-treated cochleae on days 7 and 30 were significant at multiple comparisons with Fisher's PLSD ($P < .001$ for day 7, $P = .039$ for day 30). An overall effect on data for 16 or 32 kHz of rhIGF-1 application was significant ($P < .001$ for 16 kHz, $P = .005$ for 32 kHz). The difference in threshold shifts at 16 kHz between rhIGF-1- and saline-treated cochleae was significant on day 7 ($P < .001$), but not on day 30 ($P = .051$). The difference in threshold shifts at 32 kHz between rhIGF-1- and saline-treated cochleae was significant on day 7 ($P < .001$), but not on day 30 ($P = .48$).

Histologic Protection

Immunostaining for myosin VIIa and phalloidin staining demonstrated degeneration of OHCs in the apical, middle, and basal portions of saline-treated cochleae (Fig. 2B), whereas OHC degeneration was very limited in rhIGF-1-treated cochleae (Fig. 2A). Conversely, IHC loss was not apparent in every region of both saline- and rhIGF-1-treated cochleae. Quantitative assessments revealed the significant differences in the degree of OHC loss between saline- and rhIGF-1-treated cochleae on days 7 and 30 (Fig. 3). The differences in the degree of OHC loss between the saline- and rhIGF-1-treated cochleae were significant in the apical ($P = .0006$), middle ($P < .0001$), and basal portion ($P = <.0001$) of cochleae on day 7, and in the apical ($P = .0006$), middle ($P < .0001$), and basal portion ($P = .002$) of cochleae on day 30. IHC loss was 2.7 ± 1.3% in the basal, 1.0 ± 0.5% in the middle, or 1.1 ± 0.8 in the apical portion of saline-treated cochleae, and 2.0 ±

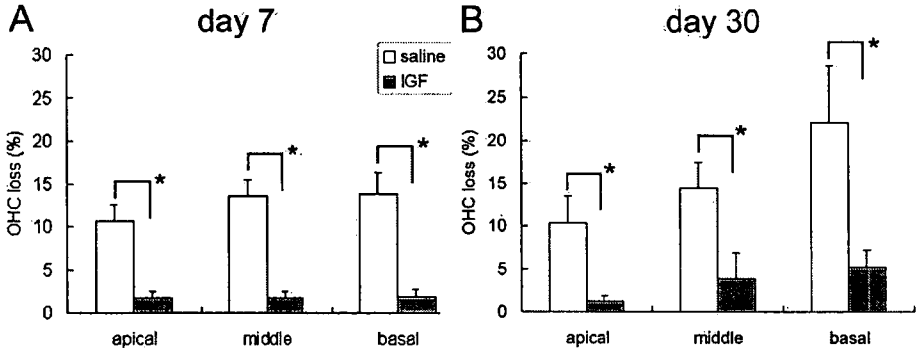

Fig. 3. Means of the percentage outer hair cell loss in the apical, middle, and basal portions of insulin-like growth factor-1- and saline-treated cochleae on days 7 (**A**) and 30 (**B**). Asterisks indicate significant differences with unpaired t test. Bars represent standard error (SE).

1.4% in the basal, 1.2 ± 0.9% in the middle, or 0.6 ± 0.6 in the apical portion of rhIGF-1-treated cochleae on day 30. No significant differences in the loss of IHCs were identified between the two experimental groups.

DISCUSSION

Our findings demonstrate that local rhIGF-1 application using a hydrogel before noise exposure has significant effects on reduction of ABR threshold shifts and of OHC loss. Our previous study has demonstrated the efficacy of local BDNF delivery to the cochlea by the biodegradable hydrogel.[3] The present findings therefore indicate that the biodegradable hydrogel can be used for local rhIGF-1 application to the cochlea. Our previous findings[3] demonstrate that high concentrations of BDNF in the cochlear fluid are maintained during days 3 to 7 after local BDNF application using this system. We then locally applied rhIGF-1 3 days before noise exposure to obtain sufficient concentrations of rhIGF-1 in the cochlear fluid. As expected, the pretreatment with rhIGF-1 demonstrated sufficient protective effects against noise trauma in the present study. However, in clinical settings, drug application after the onset of hearing loss is usually performed. Hence, we should examine the efficacy of local rhIGF-1 treatment after onset of hearing loss in the near future.

In the present study, we focused on degeneration of sensory hair cells in histologic analysis, because the degree of hair cell loss has traditionally been used to evaluate both the extent of noise-induced injury and the efficacy of protective treatments.[9,10] Quantitative assessments in the present study demonstrated significant protection of OHCs from noise trauma by local rhIGF-1 treatment. As for mechanisms of OHC protection by rhIGF-1, several possible explanations are aroused. One possible explanation is the rescue of OHCs from apoptosis resulting from noise by rhIGF-1. IGF-1 is known to inhibit apoptosis by downregulating the expression of proapoptotic genes,[11] and apoptosis is involved in OHC degeneration resulting from noise.[12] Another mechanism is the regulation of glucose transporters in OHCs by rhIGF-1. The expression of glucose transporter-5 (GLUT-5) in OHCs and its importance in their function have been reported.[13,14] GLUTs operate in the first step of glucose utilization by promoting the transport of glucose across the plasma membrane.[15] IGF-1 can regulate the expression of GLUT-5, thereby promoting neuronal cell survival.[16] Such mechanisms might be involved in the rhIGF-1-induced protection of OHCs against noise-induced injury. Further studies are required for elucidation of detailed mechanisms for the rhIGF-1-induced protection of OHCs.

ABR threshold shifts observed on day 7 remarkably recovered on day 30, whereas the damage in the organ of Corti moderately progressed until day 30. This indicates that ABR threshold shifts observed on day 7 may be caused not only by the damage in the organ of Corti, but also by reversible damages in other regions of the cochlea. In addition, the damage in the organ of Corti on day 7, 10% to 14% loss of OHCs and limited loss of IHCs, is not compatible with over 60 dB ABR threshold shifts. Recent studies have indicated involvement of damages in the cochlear lateral wall in noise-induced HL.[17] Local rhIGF-1 treatment significantly reduced ABR threshold shifts on day 7. IGF-1 has also effects on promotion of survival of fibloblasts.[18] Therefore, protective effects of IGF-1 on the fibrocytes in the spiral ligament may be involved in mechanisms for significant reduction of ABR threshold shifts on day 7.

CONCLUSION

This report demonstrates the efficacy of local rhIGF-1 application using a biodegradable hydrogel for the protection of cochleae from noise-induced hearing loss. Because the materials used in the present study are suitable for clinical application, the present findings encourage us to conduct further studies for clinical application of local rhIGF-1 treatment using the biodegradable hydrogel. However, the exact mechanisms by which rhIGF-1 acts in the cochlea are presently unclear and require further research. Furthermore, rhIGF-1 was applied before the onset of noise-induced hearing loss in the present study. The ability of rhIGF-1 to ameliorate cochlear damages when applied locally after the onset of hearing loss should therefore be examined in an experimental model in the near future.

Acknowledgments

The authors thank T. Hasson for providing the antibody for myosin VIIa.

BIBLIOGRAPHY

1. Arnold W, Senn P, Hennig M, et al. Novel slow- and fast-type drug release round-window microimplants for local drug application to the cochlea: an experimental study in guinea pigs. *Audiol Neurotol* 2005;10:53–63.
2. Tamura T, Kita T, Nakagawa T, et al. Drug delivery to the cochlea using PLGA nanoparticles. *Laryngoscope* 2005; 115:2000–2005.
3. Endo T, Nakagawa T, Kita T, et al. A novel strategy for treatment of inner ears using a biodegradable gel. *Laryngoscope* 2005;115:2016–2020.
4. Varela-Nieto I, Morales-Garcia JA, Vigil P, et al. Trophic effects of insulin-like growth factor-I (IGF-I) in the inner ear. *Hear Res* 2004;196:19–25.
5. Linseman DA, Phelps RA, Bouchard RJ, et al. Insulin-like growth factor-I blocks Bcl-2 interacting mediator of cell death (Bim) induction and intrinsic death signaling in cerebellar granule neurons. *J Neurosci* 2002;22: 9287–9297.
6. Staecker H, Van De Water TR. Factors controlling hair-cell regeneration/repair in the inner ear. *Curr Opin Neurobiol* 1998;8:480–487.
7. Malgrange B, Rigo JM, Coucke P, et al. Identification of factors that maintain mammalian outer hair cells in adult organ of Corti explants. *Hear Res* 2002;170:48–58.
8. Iwakura A, Fujita M, Kataoka K, et al. Intramyocardial sustained delivery of basic fibroblast growth factor improves angiogenesis and ventricular function in a rat infarct model. *Heart Vessels* 2003;18:93–99.
9. Keithley EM, Ma CL, Ryan AF, et al. GDNF protects the cochlea against noise damage. *Neuroreport* 1998;9: 2183–2187.
10. Shoji F, Miller AL, Mitchell A, et al. Differential protective effects of neurotrophins in the attenuation of noise-induced hearing loss. *Hear Res* 2000;146:132–142.
11. Linseman DA, Phelps RA, Bouchard RJ, et al. Insulin-like growth factor-I blocks Bcl-2 interacting mediator of cell

death (Bim) induction and intrinsic death signaling in cerebellar granule neurons. *J Neurosci* 2002;22: 9287–9297.
12. Pirvola U, Xing-Qun L, Virkkala J, et al. Rescue of hearing, auditory hair cells, and neurons by CEP-1347/KT7515, an inhibitor of c-Jun N-terminal kinase activation. *J Neurosci* 2000;20:43–50.
13. Nakazawa K, Spicer SS, Schulte BA. Postnatal expression of the facilitated glucose transporter, GLUT 5, in gerbil outer hair cells. *Hear Res* 1995;82:93–99.
14. Belyantseva IA, Adler HJ, Curi R, et al. Expression and localization of prestin and the sugar transporter GLUT-5 during development of electromotility in cochlear outer hair cells. *J Neurosci* 2000;20:RC116.
15. Bell GI, Kayano T, Buse JB, et al. Molecular biology of mammalian glucose transporters. *Diabetes Care* 1990;13: 198–208.
16. Asada T, Takakura S, Ogawa T, et al. Overexpression of glucose transporter protein 5 in sciatic nerve of streptozotocin-induced diabetic rats. *Neurosci Lett* 1998; 252:111–114.
17. Hirose K, Liberman MC. Lateral wall histopathology and endocochlear potential in the noise-damaged mouse cochlea. *J Assoc Res Otolaryngol* 2003;4:339–352.
18. Heron-Milhavet L, Karas M, Goldsmith CM, et al. Insulin-like growth factor-I receptor activation rescues UV-damaged cells through a p38 signaling pathway. *J Biol Chem* 2001;276:18185–18192.

The Laryngoscope
Lippincott Williams & Wilkins, Inc.

Drug Delivery to the Cochlea Using PLGA Nanoparticles

Tetsuya Tamura, MD; Tomoko Kita, PhD; Takayuki Nakagawa, MD, PhD; Tsuyoshi Endo, MD; Tae-Soo Kim, MD, PhD; Tsutomu Ishihara, PhD; Yutaka Mizushima, MD, PhD; Megumu Higaki, MD, PhD; Juichi Ito, MD, PhD

Objectives: **This study aimed to investigate the efficacy of encapsulating therapeutic molecules in poly lactic/glycolic acid (PLGA) nanoparticles for drug delivery to the cochlea.** ***Study Design:*** **An experimental study.** ***Methods:*** **We examined the distribution of rhodamine, a fluorescent dye, in the cochlea, liver, and kidney of guinea pigs. Intravenous injection of rhodamine or rhodamine-encapsulated PLGA nanoparticles was used to target the fluorescent dye systemically to the liver, kidney, and cochlea, and these molecules were applied locally to the round window membrane (RWM) of the cochlea. The localization of rhodamine fluorescence in each region was quantitatively analyzed.** ***Results:*** **After systemic application of rhodamine nanoparticles, fluorescence was identified in the liver, kidney, and cochlea. The systemic application of nanoparticles had a significant effect on targeted and sustained delivery of rhodamine to the liver but not the kidney or cochlea. Rhodamine nanoparticles placed on the RWM were identified in the scala tympani as nanoparticles, indicating that the PLGA nanoparticles can permeate through the RWM. Furthermore, the local application of rhodamine nanoparticles to the RWM was more effective in targeted delivery to the cochlea than systemic application.** ***Conclusions:*** **These findings indicate that PLGA nanoparticles can be an useful drug carrier to the cochlea via local application.** ***Key Words:*** **Drug delivery, nanoparticle, cochlea, inner ear, rhodamine.**
Laryngoscope, **115:2000–2005, 2005**

From the Department of Otolaryngology-Head and Neck Surgery, Kyoto University Graduate School of Medicine, Kyoto, Japan (T.T., T.K., T.N., T.E., T.-S.K., J.I.); the DDS Institute, The Jikei University School of Medicine, Tokyo, Japan (T.I., Y.M.); and the Institute of Medical Science, St Marianna University School of Medicine, Kawasaki, Japan (Y.M., M.H.).

Editor's Note: This Manuscript was accepted for publication July 20, 2005.

This study was supported by a Grant-in-Aid for Regenerative Medicine Realization from the Ministry of Education, Science, Sports, Culture and Technology of Japan.

Corresponding author: Takayuki Nakagawa, MD, PhD, Department of Otolaryngology-Head and Neck Surgery, Graduate School of Medicine, Kyoto University, Kawaharacho 54, Shogoin, Sakyo-ku, 606-8507 Kyoto, Japan. E-mail: tnakagawa@ent.kuhp.kyoto-u.ac.jp

DOI: 10.1097/01.mlg.0000180174.81036.5a

INTRODUCTION

The advancement of inner ear medicine will require the development of a means of nontraumatic and nontoxic delivery of therapeutic molecules to the cochlea. However, drug delivery to the cochlea presents a number of technical challenges, which have hindered the development of therapeutic strategies for the treatment of sensorineural hearing loss and related inner ear disorders. Reasons for the difficulty of drug delivery to the cochlea include the limited blood flow to the cochlea[1] and the existence of the blood-labyrinth barrier, which limits the transportation of molecules from blood to cochlear tissues.[2] The sustained delivery of therapeutic molecules is also critical for the efficient treatment of the cochlea, because bioactive molecules usually require a period of minutes or hours over which to produce their pharmacological actions. Consequently, a number of researchers are currently working to solve these problems and develop methods for the local application of molecules into the cochlea.[3,4]

Encapsulating bioactive molecules in nanoparticles consisting of biodegradable polymers such as poly-lactic/glycolic acid (PLGA) enables the sustained release of bioactive molecules in a controlled manner.[5] Recent advances in this field have made it possible to prepare PLGA nanoparticles using relatively simple techniques.[6] The present study aimed to examine the potential of PLGA nanoparticles for use as a vehicle for systemic and local drug delivery to the cochlea. We prepared PLGA nanoparticles encapsulating rhodamine, a red fluorescent dye, and administered these systemically or locally to adult guinea pigs. The profiles of rhodamine delivery to the cochlea were then analyzed using histologic techniques.

MATERIALS AND METHODS

Preparation of Rhodamine Nanoparticles

A PLGA formulation with a lactic/glycolic acid ratio of 50/50 was purchased from Wako Pure Chemicals Industries, Ltd. (Osaka, Japan). PLGA nanoparticles were prepared by an oil-in-water solvent diffusion method described elsewhere.[5] Briefly, a mixture of 20 μL of 0.5 mol/L zinc acetate aqueous solution and 0.7 mL of acetone dissolved in 20 mg of PLGA (Mw 8000) and 1 mg of rhodamine B (Sigma Chemical Co., St. Louis, MO) was added to 5 mL of a 0.5% (w/v) egg yolk lecithin (Sigma) aqueous

suspension. To chelate the zinc, 1 mL of 0.5 mol/L EDTA aqueous solution (pH 7.5) was added to the resulting suspension of nanoparticles. The nanoparticles were purified from unencapsulated rhodamine by ultrafiltration (YM-50, Millipore Co., Bilenica, MA) and subsequent gel filtration (PD-10 column, Amersham Biosciences, Tokyo, Japan). The diameter of the nanoparticles ranged from 140 to 180 nm.

Animals

Pigmented guinea pigs weighing 250 to 300 g were purchased from Japan SLC Inc. (Hamamatsu, Japan) for use in this study. The Animal Research Committee, Graduate School of Medicine, Kyoto University approved all experimental protocols, and animal care was supervised by the Institute of Laboratory Animals, Graduate School of Medicine, Kyoto University. All experimental procedures were performed in accordance with National Institutes of Health (NIH) guidelines for the care and use of laboratory animals.

Systemic Application

Experimental animals were anesthetized with ketamine (20 mg/kg IM; Sankyo Co., Tokyo, Japan) and xylazine (5 mg/kg IM; Bayer, Tokyo, Japan). We exposed the right femoral vein and injected PLGA nanoparticles encapsulating rhodamine B (nanoRho; 0.25 mL, 20 μg/mL physiological saline) into 12 animals and normal, unencapsulated rhodamine B (Rho; 0.25 mL, 20 μg/mL physiological saline) into eight animals. At 10 or 120 minutes after injection of rhodamine, the animals were killed by cervical rotation under anesthesia with a lethal dose of ketamine and xylazine. The left temporal bones, kidney, and liver were immediately excised from the animals. The cochleae were dissected in cold 0.01-mol/L phosphate-buffered saline at pH 7.4 (PBS), and the kidney and liver were cut into approximately 1 cm^3 blocks. The specimens were immersed in 10% trichloroacetic acid in PBS at 4°C for 24 hours. After washing with PBS, specimens were embedded in OCT compound (Tissue-Tek, Sakura Finetechnical, Tokyo, Japan) and frozen at −80°C until use.

Local Application

Under general anesthesia with ketamine and xylazine, the bulla of the left temporal bone was exposed using a retroauricular approach. A small hole was made on the bulla to expose the round window membrane (RWM). A piece of gelfoam immersed with nanoRho (0.25 mL, 20 μg/mL physiological saline) was placed on the RWM of four animals. The same amounts of unencapsulated Rho were applied to another four animals. The cochleae were then collected 24 hours after application. Tissue preparation was performed according to the procedure described above for samples from systemically treated animals. To examine the dynamics of these molecules in the cochlea, we used a glass pipette to inject 10 μL of nanoRho through the RWM into the scala tympani of three animals, at the same concentration as that placed on the RWM. The temporal bones were collected 24 hours after the injection and used for histologic analysis.

Analysis of Rhodamine Distribution

Tissue specimens were cut into 10-μm thick sections. Four mid-modiolus sections from the cochleae of each animal were used for histological analysis. The specimens were covered with Vector Shield (Vector Laboratories Inc., Burlingame, CA), and viewed with a Nikon ECLIPSE E600 fluorescence microscope (Nikon, Tokyo, Japan). We counted the number of red fluorescent rhodamine particles within the cochlea in every section and calculated the mean number of particles from four sections, for each animal, for statistical analyses.

Four randomly selected sections from the liver and kidney of each animal were also used for histologic analysis. The numbers of rhodamine particles in five random fields of 0.4 mm^2 were counted in each section. The mean number of rhodamine particles from the four sections was determined for each animal.

Statistics

We calculated the differences in the numbers of red fluorescent particles between nanoRho and Rho at 10 or 120 minutes after systemic application. The Mann-Whitney *U* test was used for all statistical calculations, and a probability (*P*) value of less than 0.05 was considered to be significant. Values are expressed as mean ± SE.

RESULTS

Liver and Kidney

In the liver, rhodamine fluorescence was found in every experimental group (Fig. 1). Rhodamine fluorescence was observed as moderate red fluorescent dots following application of Rho (Fig. 1C), and as intense red fluorescent dots following nanoRho application (Fig. 1A, B). A number of red fluorescent dots were observed at 10 minutes after Rho application (74.5 ± 4.5), but this figure had decreased significantly to 8.5 ± 0.6 at 120 minutes ($P = 0.0008$, Fig. 2A). Numerous red fluorescent dots were found in the liver after nanoRho application: 542.4 ± 61.2 at 10 minutes and 533.8 ± 24.8 at 120 minutes (Fig. 2A). There was no significant difference in numbers of red fluorescent dots between these two time points, indicating that the PLGA nanoparticles promoted sustained delivery of rhodamine to the liver. The application of nanoRho resulted in significantly higher numbers of red fluorescent dots in the liver than were seen after Rho application, at 10 ($P = 0.0002$) and 120 minutes ($P = 0.0002$) after application (Fig. 2A), showing that PLGA nanoparticles are significantly more effective at targeting delivery of Rho to the liver.

In the kidney, few or no red fluorescent dots were identified after application of Rho (10 min: 0.3 ± 0.3, 120 min: 0; Fig. 1D, 2B) or nanoRho (10 min: 4.4 ± 2.0, 120 min: 0.2 ± 0.2; Fig. 2B). There was no significant difference in the number of red fluorescent dots in the kidney between 10 and 120 minutes for either Rho or nanoRho application, or between these two preparations of Rho. These findings indicate that PLGA nanoparticles have no significant impact on the effectiveness of targeted delivery of rhodamine to the kidney.

Cochleae after Systemic Application

In the cochlea, no red fluorescent dots were observed after systemic application of Rho, whereas they were observed after systemic application of nanoRho (Fig. 1E-H). Rhodamine particles were localized in spiral prominence (Fig. 1E), stria vascularis (Fig. 1F), or the cochlear melodious (Fig. 1G, H). The regions in which rhodamine particles were localized corresponded to the location of blood vessels in the cochlea. Rhodamine fluorescence was found in the apical, middle, and basal portion of the cochlea. The number of red fluorescent dots after nanoRho application was 2.8 ± 0.3 at 10 minutes and 0.1 ± 0.1 at 120 minutes (Fig. 2C), and the difference between 10 and 120 minutes was significant at $P < 0.0001$. The numbers of rhodamine

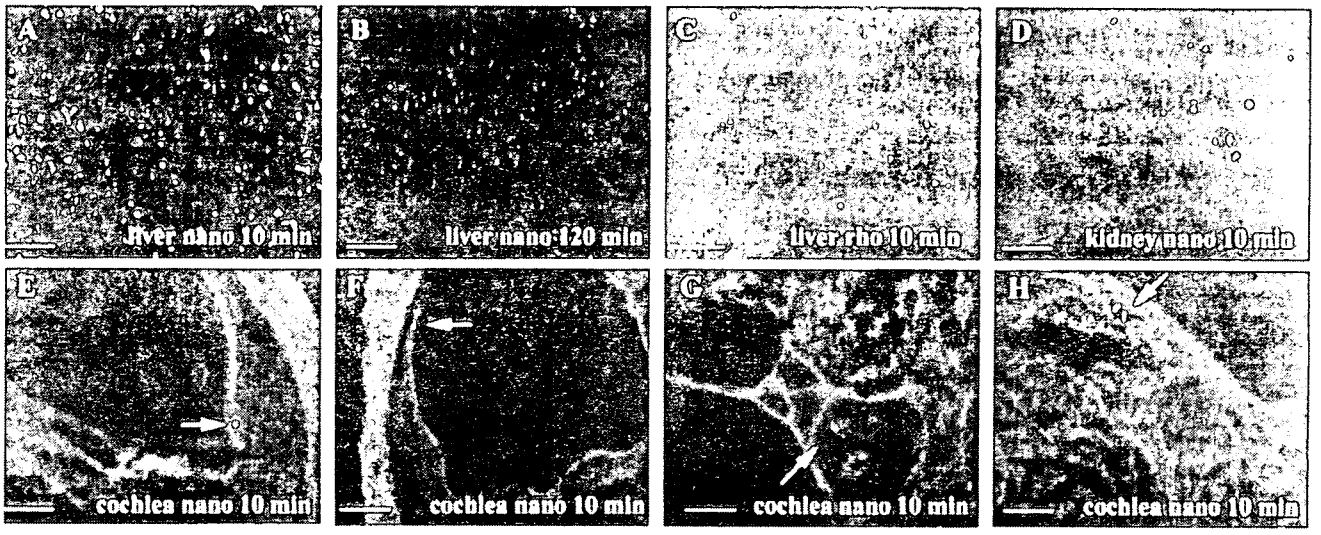

Fig. 1. Localization of rhodamine fluorescence in the liver, kidney, and cochlea after systemic application of rhodamine-nanoparticles or rhodamine Rhodamine fluorescence is frequently observed in the liver at 10 (**A**) and 120 minutes (**B**) after application of rhodamine-nanoparticles (nano). Rhodamine fluorescence is also identified in the liver at 10 minute after rhodamine (rho) application (**C**). A few dots with fluorescence are found in the kidney (**D**) and cochlea (**E-H**). In cochleae, rhodamine fluorescence is identified in the spiral prominence (arrow in E), stria vascularis (arrow in **F**), and modiolus (arrows in **G, H**). Scale bars represent 50 μm.

particles following systemic application of nanoRho were significantly higher than those following systemic application of Rho at 10 minutes (P = 0.0001), but not at 120 minutes (P = 0.4142; Fig. 2C).

Cochleae after Local Application

Following a local injection of nanoRho into the scala tympani, numerous rhodamine particles showing strong red fluorescence were found distributed from the base to the apex of the cochlea 24 hours after application (Fig. 3A). Rhodamine particles were located in the scala tympani and vestibule. After the application of nanoRho to the RWM, rhodamine fluorescence was found in the scala tympani of the basal and middle portion of the cochlea (Fig. 3C, D). The majority of rhodamine particles were located in the basal portion. The number of red fluorescent dots in the cochlea was 28.8 ± 4.5 after local nanoRho application on the RWM. There were residual rhodamine particles on the RWM (Fig. 3B), which showed intense fluorescence as well as those in the scala tympani. The number of rhodamine particles after local application of nanoRho was approximately 10-fold higher than that at 10 minutes after systemic application. Conversely, no rhodamine fluorescence was found in the cochlea after local application of unencapsulated Rho.

DISCUSSION

Most of the drugs for the treatment of inner ear diseases have been administered systemically. We then evaluated the effects of PLGA nanoparticles on drug delivery to the cochlea via systemic application. We used the liver as a control organ to analyze the distribution of rhodamine nanoparticles after systemic application, because the liver has a good blood supply, with abundant phagocytes, in which nanoparticles have a characteristic tendency to accumulate.[7] The presence of rhodamine fluorescence in the liver following systemic application of either nanoRho or Rho confirms the accuracy of systemic application of these molecules. The numbers of rhodamine fluorescence dots in the liver after application of nanoRho were significantly higher than those after application of Rho. Furthermore, the levels of fluorescence after the administration of nanoRho showed no significant decrease at 120 minutes after application, indicating targeted and sustained delivery of rhodamine to the liver by encapsulating PLGA nanoparticles. In contrast to the liver, no significant effects of PLGA nanoparticles on the delivery of rhodamine to the kidney were found in the present study. The differences in the distribution of rhodamine particles to the liver and kidney might be caused by the organ-specific characteristics, including the distribution of phagocytes.

The blood flow to the liver or kidney is much higher than that for the cochlea.[8] Rhodamine particles were found in the cochlea after systemic application of nanoRho, despite the presence of a small blood supply to this organ, suggesting the efficacy of PLGA nanoparticles for drug delivery to the cochlea. However, few rhodamine particles in the cochlea were identified 120 minutes after systemic application. The present findings also indicate that rhodamine particles observed in the cochlea are located in cochlear vessels. The PLGA nanoparticles used in the present study can take a couple of days to release 50% of the molecules they contain.[5] Consequently, rhodamine particles located in the cochlear vessels at 10 minutes after application might be removed via cochlear blood flow within 120 minutes. These findings indicate that systemic application of PLGA nanoparticles might not have significant effects on cochlear drug delivery under physiologic conditions.

Rhodamine particles were identified in the cochlea 24 hours after local application of nanoRho. PLGA is a bio-

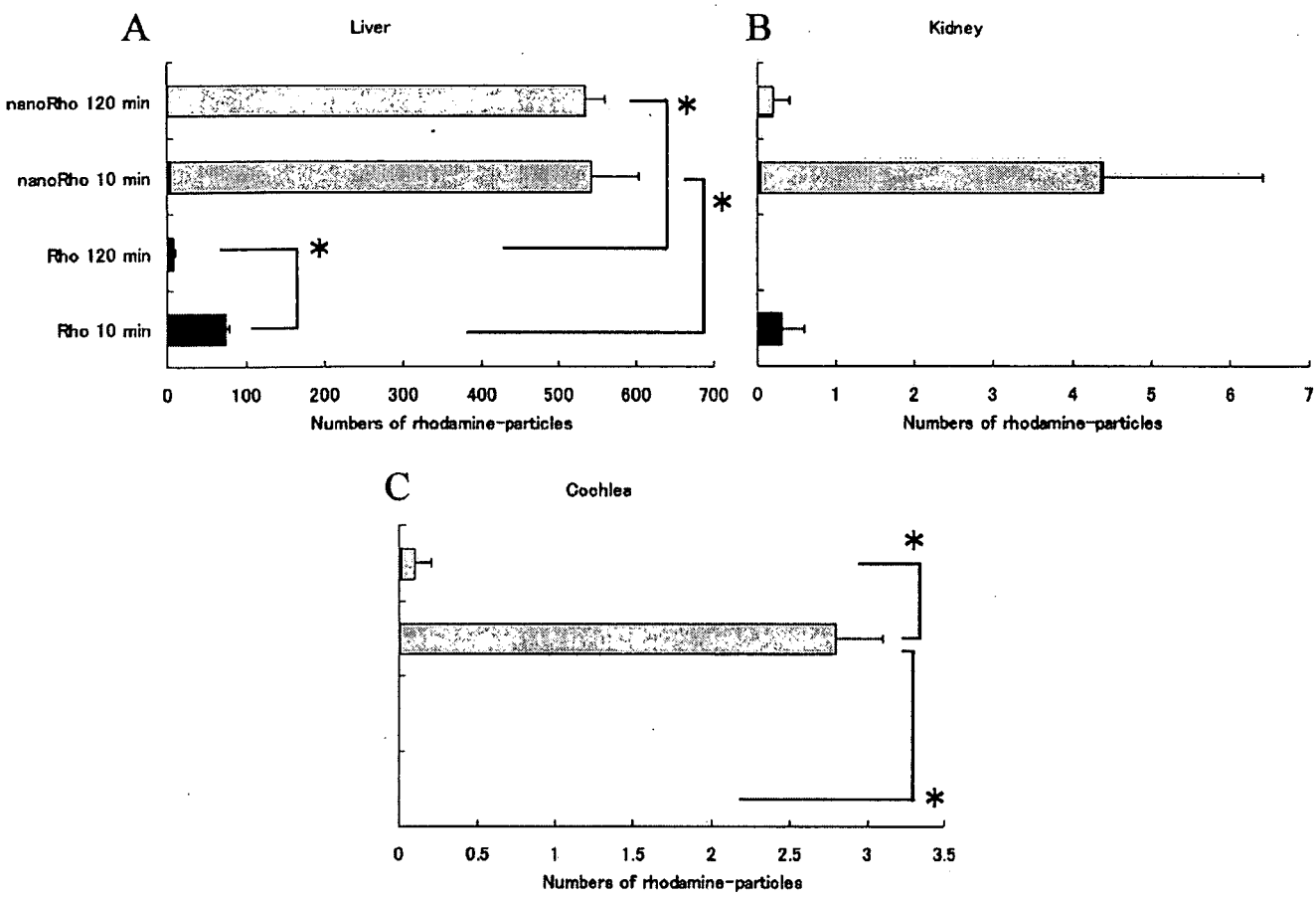

Fig. 2. The mean numbers of rhodamine particles in the liver, kidney, and cochlea at 10 or 120 minutes after systemic application of rhodamine nanoparticles (nanoRho) or normal rhodamine (Rho). The x-axis indicates the numbers of rhodamine-particles in 0.4 mm^2 for the liver and kidney and those in one section for the cochleae. Bars represent standard errors. Asterisks indicate statistical significance ($P < 0.005$, Mann-Whitney test).

degradable polymer, so rhodamine can be released from nanoparticles in both the middle and the inner ear. Rhodamine particles observed in the cochlea after local nanoRho application exhibited strong fluorescence, similar to that seen after systemic nanoRho application. Residual rhodamine particles on the RWM also exhibited strong red fluorescence. In addition, PLGA nanoparticles are small enough to pass through the RWM.[9] Therefore, the rhodamine fluorescence observed in the cochlea after local application of nanoRho application may result from rhodamine nanoparticles that have passed through the RWM and not from rhodamine released from PLGA nanoparticles in the middle ear. Previous studies have demonstrated that cochlear fluids have an extremely slow flow rate.[10] Rhodamine particles observed in the cochlea after local nanoRho application were located in the perilymphatic space, which indicates that the clearance of rhodamine particles depends on the flow of perilymph. If the flow of perilymph is slow, it would follow that the clearance of rhodamine particles from the cochlea might also be slow, thereby resulting in sustained release of rhodamine from rhodamine particles in the perilymph. In addition, the numbers of rhodamine particles in the cochlea after local nanoRho application are apparently higher than those after systemic application. Therefore, the local application of PLGA nanoparticles to the RWM may be an effective strategy for targeted and sustained drug delivery to the cochlea.

Rhodamine fluorescence was found from the basal to apical portion of the cochlea after a local injection of nanoRho into the scala tympani, whereas it was observed only to a limited degree in the basal portion of the cochlea after direct application of nanoRho to the RWM. The distribution of molecules within the cochlear fluid spaces is dominated by passive diffusion,[11] the rate of which depends on the physiologic characteristics of the molecules, particularly molecular weight.[12] Therefore, rhodamine released from PLGA nanoparticles in the perilymphatic space possibly spreads more toward the apical portions of the cochlea than PLGA nanoparticles applied to the RWM. Further studies are required to optimize the profile of nanoparticles in accordance with the desired distribution and release of drugs they contain.

Various therapeutic molecules for inner ear diseases can be encapsulated in PLGA nanoparticles and applied as intratympanic drugs. The efficacy of encapsulating betamethasone phosphate in PLGA nanoparticles has already been confirmed using animal models for rheumatoid

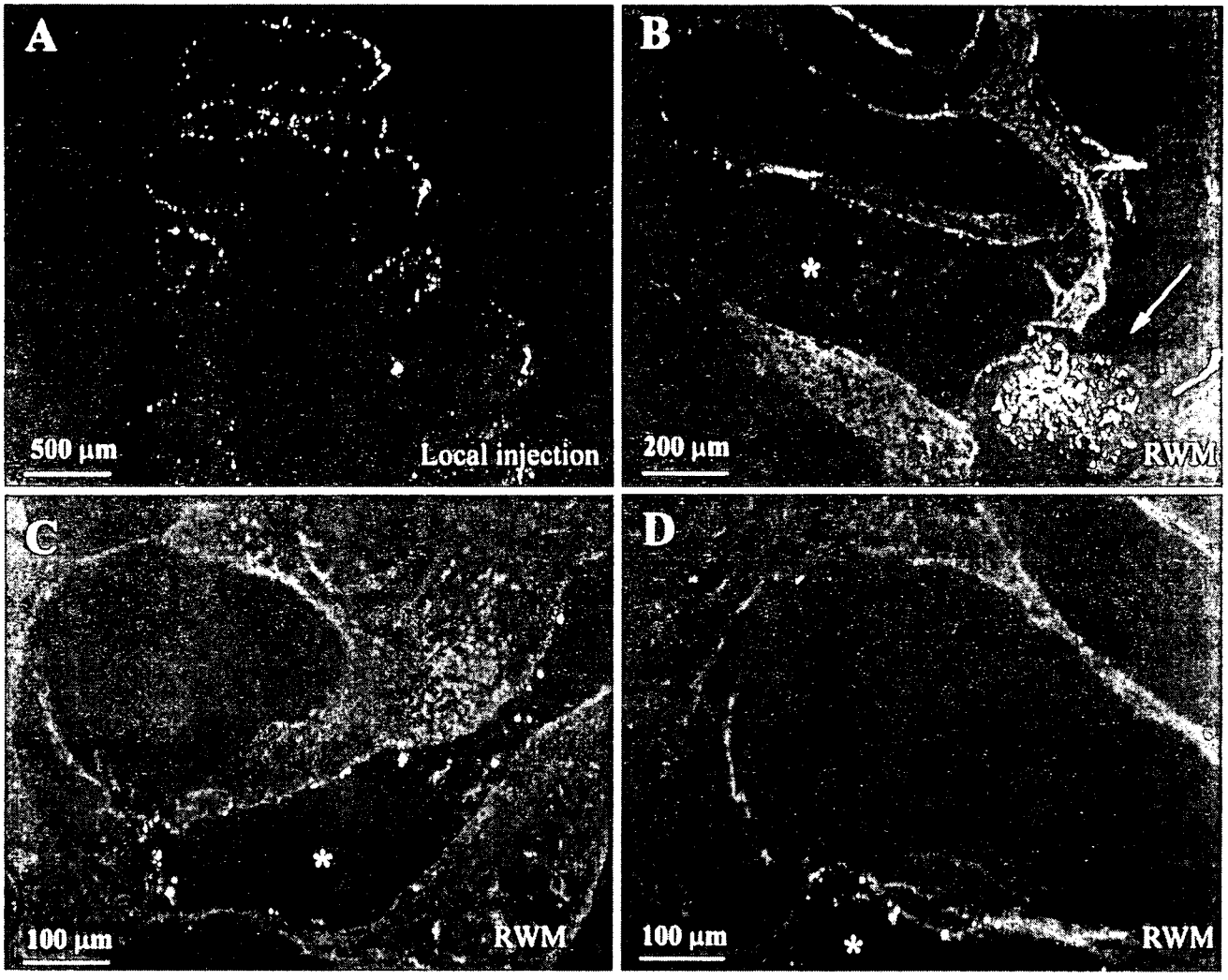

Fig. 3. Localization of rhodamine-particles in cochleae after local application of rhodamine nanoparticles After a local injection of rhodamine-nanoparticles into the scala tympani, numerous rhodamine-particles are found distributed from the basal to the apical portion of the cochlea (**A**). Rhodamine particles are identified in the scala tympani of the basal portion of cochleae after application of rhodamine-nanoparticles on the round window membrane (asterisks in **B–D**). Residual rhodamine particles on the round window membrane are indicated by an arrow (**B**). Scale bars represent 500 μm in **A**, 200 μm in **B**, and 100 μm in **C** and **D**.

arthritis.[13] Local gentamicin application has been used for the control of intractable vertigo in Ménière disease.[14] PLGA nanoparticles can be utilized for controlled release of gentamicin. Given these findings, we intend to examine the effects of PLGA nanoparticles encapsulating therapeutic molecule on models of inner ear diseases.

CONCLUSIONS

In the present study, rhodamine nanoparticles were identified in the cochlea after systemic or local application, suggesting that PLGA nanoparticles have a potential use in drug delivery to the cochlea. The transfer of PLGA nanoparticles through the RWM to the perilymph was also demonstrated, indicating the efficacy of encapsulating drugs in PLGA nanoparticles as a strategy for sustained and targeted drug delivery to the cochlea.

Acknowledgments

This study was supported by a Grant-in-Aid for Regenerative medicine realization project from the Ministry of Education, Science, Sports, Culture and Technology of Japan.

BIBLIOGRAPHY

1. Angelborg C, Hillerdal M, Hultcrantz E, Larsen HC. The microsphere method for studies of inner ear blood flow. *ORL J Otorhinolaryngol Relat Spec.* 1998;50:355–362.
2. Juhn SK, Hunter BA, Odland RM. Blood-labyrinth barrier and fluid dynamics of the inner ear. *Int Tinnitus J* 2001; 7:72–83.
3. Lefebvre PP, Staecker H. Steroid perfusion of the inner ear for sudden sensorineural hearing loss after failure of conventional therapy: a pilot study. *Acta Otolaryngol* 2002; 122:698–702.
4. Kawamoto K, Sha SH, Minoda R, et al. Antioxidant gene

therapy can protect hearing and hair cells from ototoxicity. *Mol Ther* 2004;9:173–181.
5. Ishihara T, Izumo N, Higaki M, et al. Role of zinc in formulation of PLGA/PLA nanoparticles encapsulating betamethasone phosphate and its release profile. *J Control Release* 2005;105:68–76.
6. Murakami H, Kobayashi M, Takeuchi H, Kawashima Y. Preparation of poly (DL-lactide-co-glycolide) nanoparticles by modified spontaneous emulsification solvent diffusion method. *Int J Pharm* 1999;187:143–152.
7. Mizushima Y, Hamano T, Yokoyama K. Tissue distribution and anti-inflammatory activity of corticosteroids incorporated in lipid emulsion. *Ann Rheum Dis* 1982;41:263–267.
8. Shinomori Y, Spack DS, Jones DD, Kimura RS. Volumetric and dimensional analysis of the guinea pig inner ear. *Ann Otol Rhinol Laryngol* 2001;110:91–98.
9. Goycoolea MV. Clinical aspects of round window membrane permeability under normal and pathological conditions. *Acta Otolaryngol* 2001;121:437–447.
10. Ohyama K, Salt AN, Thalmann R. Volume flow rate of perilymph in the guinea-pig cochlea. *Hear Res* 1988;35:119–129.
11. Salt AN, Ma Y. Quantification of solute entry into cochlear perilymph through the round window membrane. *Hear Res* 2001;154:88–97.
12. Hobbie RK. Transport in an infinite medium. In: Hobbie RK (eds). *Intermediate Physics for Medicine and Biology*. New York: Springer; 1997. pp 85–90.
13. Higaki M, Ishihara T, Izumo N, Takatsu M, Mizushima Y. Treatment of experimental arthritis with poly(D,L-lactic/glycolic acid) nanoparticles encapsulating betamethasone sodium phosphate. *Ann Rheum Dis* 2005;64:1132–1136.
14. Minor LB. Intratympanic gentamicin for control of vertigo in Meniere's disease: vestibular signs that specify completion of therapy. *Am J Otol* 1999;20:209–219.

The Laryngoscope
Lippincott Williams & Wilkins, Inc.

Novel Strategy for Treatment of Inner Ears using a Biodegradable Gel

Tsuyoshi Endo, MD; Takayuki Nakagawa, MD, PhD; Tomoko Kita, PhD; Fukuichiro Iguchi, MD, PhD; Tae-Soo Kim, MD, PhD; Tetsuya Tamura, MD; Koji Iwai, MD; Yasuhiko Tabata, PhD; Juichi Ito, MD, PhD

Objective: **The present study aimed to evaluate the efficacy of a biodegradable hydrogel as a drug-delivery medium for the inner ear. Brain-derived neurotrophic factor (BDNF) was chosen as the agent to be administered.** ***Method:*** **First, we used an enzyme-linked immunosorbent assay to measure BDNF concentrations in the cochlear fluid after placing a hydrogel containing this agent onto the round-window membrane of the ear. Second, the functional and histologic protection of the auditory primary neurons (spiral ganglion neurons [SGNs]) by BDNF applied through the hydrogel was examined using an animal model of SGN degeneration.** ***Results:*** **The results revealed sustained delivery of BDNF into the cochlear fluid by way of the hydrogel. Second, the functional and histologic protection of the auditory primary neurons (SGNs) by BDNF applied through the hydrogel was examined using an animal model of SGN degeneration. The measurement of electrically evoked auditory-brainstem responses demonstrated that BDNF delivered by way of the hydrogel significantly reduced the threshold elevation. Immunohistochemistry for neurofilament 200 kD demonstrated increased survival of SGNs because of BDNF application through the hydrogel.** ***Conclusion:*** **These findings indicate that biodegradable hydrogels can be used for drug delivery to the inner ear.** ***Key Words:*** **Drug delivery, HL, inner ear, neurotrophins, protection.**

Laryngoscope, **115:2016–2020, 2005**

From the Department of Otolaryngology–Head and Neck Surgery, Graduate School of Medicine (T.E., T.N., T.K., T.-S.K., T.T., K.I., J.I.), the Institute for Frontier Medical Science (Y.T.), Kyoto University, Kyoto, Japan, and the Department of Otolaryngology, Otsu Red Cross Hospital (F.I.), Otsu, Japan.

Editor's Note: This manuscript was accepted for publication August 10, 2005.

This study was supported by a Grant-in-Aid for Regenerative Medicine Realization from the Ministry of Education, Science, Sports, Culture and Technology of Japan.

A part of this study was presented at the 40th Workshop on Inner Ear Biology, Granada, Spain, September 8–10, 2003 and the 27th Midwinter meeting for the Association for Research in Otolaryngology, Daytona Beach, Florida, U.S.A., February 21–26, 2004.

Send Correspondence to Dr. Takayuki Nakagawa, Department of Otolaryngology–Head and Neck Surgery, Graduate School of Medicine, Kyoto University, Kawaharacho 54, Shogoin, Sakyo-ku, 606-8507 Kyoto, Japan. E-mail: tnakagawa@ent.kuhp.kyoto-u.ac.jp

DOI: 10.1097/01.mlg.0000183020.32435.59

INTRODUCTION

Sensorineural hearing loss (SNHL) is one of the most common disabilities in industrial countries. However, therapeutic strategies for the treatment of SNHL are limited to hearing aids and cochlear implants. Excessive noise, ototoxic drugs, genetic disorders, and aging can all cause SNHL. Previous studies on human temporal bones and animal models have indicated that the loss of cochlear hair cells and cochlear neurons (spiral ganglion neurons [SGNs]) are among the major causes of SNHL.[1] Loss of auditory function caused by the degeneration of auditory hair cells can be partly restored by cochlear implants, which are small devices that are surgically implanted into the inner ear to stimulate SGNs. However, the success of these implants depends on the remaining SGNs, and their loss severely compromises the efficacy of this technique.[2] Protecting these cells from irreversible degeneration is therefore of primary importance.

The problem of how to deliver drugs to the inner ear has been a considerable obstacle to the development of treatments for inner ear degeneration. The systemic application of drugs carries the risk of unwanted side effects. In addition, the blood–inner ear barrier, which inhibits the transport of drugs from the serum to the inner ear, represents a fundamental obstacle to systemic application.[3] The inner ear tissues are isolated from the surrounding organs by a bony construction, which allows the topical introduction of drugs by local application. On the basis of these considerations, local application has generally been used for drug application to the inner ear. The inner ear is connected to the middle ear cavity by the round-window membrane (RWM). Drug application through the RWM has therefore been exploited as a route for the local application of drugs to the inner ear; this approach has been reported for the clinical application of both steroids[4] and gentamicin.[5] However, this technique has not been widely used in a clinical setting because controlled, noninvasive delivery systems have not yet been developed.

A biodegradable hydrogel has been developed for the sustained delivery of proteins, including growth and trophic factors.[6–8] In this approach, a positively charged protein is electrostatically complexed with negatively charged polymer chains, which are components of the

biodegradable hydrogel. Biodegradation of the polymer chains leads to release of the protein, which is regulated by changes that occur during the degradation process. The efficacy of this drug-delivery system has been demonstrated for the release of basic fibroblast growth factor for angiogenesis[7] and bone morphogenetic protein 1 for bone formation.[8]

In the present study, we examined whether biodegradable hydrogels could be used for the sustained delivery of brain-derived neurotrophic factor (BDNF), which is known to promote the survival of SGNs,[9,10] to the inner ear by way of the RWM.

MATERIALS AND METHODS

Experimental Animals

Pigmented guinea pigs weighing 250 to 300 g were purchased from Japan SLC, Inc., (Hamamatsu, Japan) for use in this study. Animal care was carried out under the supervision of the Institute of Laboratory Animals of the Graduate School of Medicine, Kyoto University, Japan.

Biodegradable Hydrogels

Biodegradable hydrogels were prepared as described previously.[6–8] They were generated through the glutaraldehyde cross-linking of porcine type-I collagen (Gunze, Ayabe, Japan). The rates of degradation were determined according to the concentration of glutaraldehyde. We used the hydrogel generated with 60 0mol/L glutaraldehyde in this study.

BDNF Concentrations in Perilymph

Pigmented guinea pigs were anesthetized with ketamine (20 mg/kg, intramuscularly [IM]; Sankyo Co., Tokyo, Japan) and xylazine (5 mg/kg, IM; Bayer, Tokyo, Japan). A hydrogel immersed with BDNF (84 μg dissolved in 2 μL physiologic saline) was positioned on the RWM of each animal in the treated group (n = 20). For animals in the control group (SAL, n = 20), a hydrogel immersed with physiologic saline alone was placed on the RWM. Finally, animals in the injection group (n = 20) received an injection of BDNF (84 μg dissolved in 2 μL physiologic saline) through the RWM. The perilymph was collected on day 3 or 7 after the drug application to measure the BDNF concentration. For each animal, a small hole was made in the basal turn of the cochlea 2 mm from the RWN, under general anesthesia, and 2 μL of the perilymph was collected through the hole using a micropipette. BDNF proteins in the perilymph (10 μL from 5 animals) were quantified using an enzyme-linked immunoadsorbent assay (ELISA). The ELISA was performed using a BDNF Emax Immunoassay System kit according to standard protocols (Promega, Madison, WI). The triplicates were averaged, and the values were corrected for the total amount of protein in the sample. Values for BDNF protein levels were expressed as pg/mg of total protein.

Functional Protection

An animal model of the degeneration of SGNs[10,11] was used to evaluate the functional and morphologic protection of SGNs induced by the application of BDNF through a biodegradable hydrogel. The functionality of the cochleae was assessed using the electrically evoked auditory brain-stem response (eABR). Pigmented guinea pigs received an IM injection of kanamycin (KM; 400 mg/kg; Wako Pure Chemical Industries, Ltd., Osaka, Japan) and an intravenous injection of ethacrynic acid (EA; 25 mg/kg; Wako Pure Chemical Industrie,s Ltd) to induce the total loss of cochlear hair cells, resulting in the secondary degeneration of SGNs. On day 18, after the KM and EA treatment, the eABR thresholds were measured in four animals without drug application. For animals in the SAL group, a hydrogel immersed with 2 μL physiologic saline was positioned on the RWM on day 18 (n = 12). In the BDNF group, a hydrogel immersed in BDNF (84 μg dissolved in 2 μL physiologic saline) was placed on the RWM of each animal (n = 12). Measurement of the eABR thresholds was performed 3 or 7 days after drug application (n = 4 in each case) using the method described by Hall.[12] The eABRs typically demonstrated a classic waveform consisting of five positive waves, and thresholds were determined using wave III. The threshold was defined as the lowest stimulus level in 50 μA steps that evoked a replicable waveform.

Histologic Protection

Histologic protection was evaluated on the basis of the cell densities of surviving SGNs in the Rosenthal's canals. On day 7 after drug application, the animals were deeply anesthetized with a lethal dose of ketamine and xylazine and were perfused intracardially with physiologic saline followed by 4% paraformaldehyde in 0.01 mol/L phosphate-buffered saline at pH 7.4. Four temporal bones were collected from each experimental group and immersed in the same fixative at 4°C for 12 hours. Specimens were prepared as cryostat sections (thickness 10 μm) after decalcification with 0.1 mol/L ethylenediamine tetra-acetic acid for 14 days at 4°C. Four mid-modiolus sections were chosen from each cochlea and stained by immunohistochemistry for neurofilament (NF) 200 kD and peripherin: the former was used as a marker for neurons and the latter as a marker for type II SGNs.[13] Anti-NF mouse monoclonal antibody (1:500; Sigma, St. Louis, MO) and antiperipherin rabbit polyclonal antibody (1:200; Chemicon, Temecula, CA) were used as primary antibodies. Fluorescein isothiocyanate-conjugated antimouse goat antibody (1:400; Santa Cruz Biotechnology, Santa Cruz, CA) and rhodamine-conjugated antirabbit donkey antibody (1:500; Chemicon) were used as secondary antibodies. Counterstaining by DAPI (Molecular Probes, Eugene, OR) was performed at the end of the staining procedures. Nonspecific labeling was tested by omitting the primary antibody from the staining procedures. The specimens were viewed with a Nikon ECLIPSE E600 fluorescence microscope (Nikon, Tokyo, Japan). Both NF- and DAPI-positive cells located in the Rosenthal's canal were defined as SGNs, and peripherin-positive cells were regarded as type II SGNs. The numbers of SGNs and type II SGNs were counted in each turn of the cochleae. The area of the Rosenthal's canal was measured on bright-field images using NIH image software (version 1.62; http://rsb.info.nih.gov/nih-image). The density of SGNs and type II SGNs was then calculated. The average of the densities from four sections was defined as the data point for each animal.

Statistical Analyses

Two-factor factorial analysis of variance was used to determine the statistical significance differences between the BDNF concentrations in the perilymph and the eABR thresholds among the experimental groups. A pair-wise comparison was performed using multiple comparisons with the Tukey-Kramer test. Differences in SGN or type II SGN densities in each turn of the cochleae among the experimental groups were examined using unpaired t tests. For all analyses, a probability (P) value less than .01 was considered to be statistically significant. Values are expressed as mean $\pm$ SD.

RESULTS

BDNF Concentrations in Perilymph

The BDNF concentrations in the perilymph of the SAL and injection groups were either extremely low or